NOAA Technical Memorandum NWS TC 1

AN OUTLINE OF SEVERE LOCAL STORMS WITH THE MORPHOLOGY OF ASSOCIATED RADAR ECHOES

Rockville, Md.
June 1982

U.S. DEPARTMENT OF COMMERCE / National Oceanic and Atmospheric Administration / National Weather Service

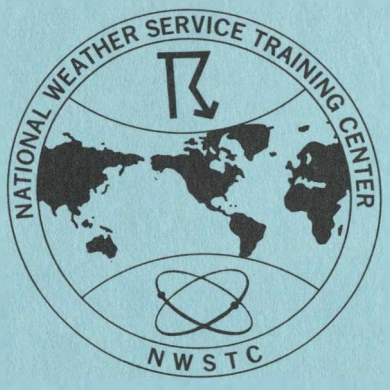

NATIONAL OCEANIC AND ATMOSPHERIC ADMINISTRATION

NATIONAL WEATHER SERVICE TRAINING CENTER

NATIONAL WEATHER SERVICE TRAINING CENTER TECHNICAL MEMORANDA

The National Weather Service Training Center, Kansas City, Missouri, is responsible for providing instruction to meet most of the training needs of the National Weather Service. Courses are developed and conducted by two divisions of the Training Center—Meteorology and Management, and Electornics and Engineering.

Instructors maintain close contact with the research community, top management in the NWS, and suppliers of NWS equipment to remain current in the state of the art of their subjects and with national policy. Course material is constantly developed and revised to provide students with the most accurate and up-to-date information. Some of this material is suitable for adoption as Technical Memoranda. Publication of Technical Memoranda by National Weather Service Training Center will be a function of usefulness of data, needs of operational offices and instructors' time. Constructive comments from users are invited.

NOAA Technical Memorandum NWS TC 1

AN OUTLINE OF SEVERE LOCAL STORMS WITH THE MORPHOLOGY OF ASSOCIATED RADAR ECHOES

Robert Grebe
National Weather Service Training Center
Kansas City, Mo.

Rockville, Md.
June 1982

UNITED STATES
DEPARTMENT OF COMMERCE
Malcolm Baldrige, Secretary

National Oceanic and
Atmospheric Administration
John V. Byrne, Administrator

National Weather
Service
Richard E. Hallgren, Director

PREFACE

Preliminary results of a three year study by Pearson (1979) indicated that 95 out of every 100 tornado warnings issued by the National Weather Service were unsuccessful. Pearson's verification technique classified a warning as a hit if it was issued prior to the beginning of the tornado in each affected county. For example, if a tornado began at 5:30 and you issued a warning at 5:32, it was classified as a miss for that county.

The need to improve the accuracy of our severe local storm warnings is a goal common to us all. The technique of improving warnings is dependent upon our ability to identify the potential before the event occurs. The primary tools at our disposal include trained spotters, satellite and radar observations.

This outline focuses on the interpretation of conventional radar data for the identification of severe local storms. It is an update of classical papers by Donaldson (1965) and Hamilton (1969). Also included are techniques for analyzing video integrated and processed (VIP) radar data proposed by Lemon (1980).

Most of the radar research work in severe local storms accomplished in the 1970's was done with Doppler radar. Doppler is conventional radar plus "more". The "more", velocity derived fields, has increased our understanding of storm structure and the morphology of precipitation related echoes. It will be to the advantage of the operational community using conventional radar to apply the technology of Doppler in a practical way.

Documented radar signatures associated with severe local storms dating back to the 1950's have been included. Some of them are in apparent conflict with contemporary storm models. The rationale for including them is (1) these signatures can still be operationally useful as alerting features and (2) today's storm models are likely to change as our understanding of the physical processes that produces them increases. As such, this outline is not intended to conflict with National or Regional National Weather Service policy regarding the use of radar signatures in issuing severe thunderstorm or tornado warnings.

The test of a radar signature leading to the identification of a severe local storm occurs in the field under the stress of making day-to-day warning decisions. No signature or combination of signatures guarantees the existence of a severe storm any more than a numerical model will produce a perfect weather forecast. In both cases, a probability is assigned to the occurrence of the event and a decision is based on that probability. Objective evaluators for some of the signatures defined by Donaldson, et al. (1975) have been included.

I selected the opening quote from my missed friend and colleague, Clarence David, because it addresses the need to improve the accuracy of our severe local storm forecasts and warnings. Not only do we need to know when to worry but equally important when not to worry. The decision not to issue a warning is often the hardest one of all to make.

"The trick to forecasting severe thunderstorms is to know when to worry."

Clarence David

DEDICATED

to the memory
and extraordinary
severe local storms
forecasting ability
of

CLARENCE L. DAVID
(1926-1979)

whose tornado forecasts of April 3, 1974,
were the pinnacle of the state-of-the-art.
It was clearly a time to worry!

ACKNOWLEDGMENTS

The author specifically wishes to express his sincere appreciation for the critical review and valuable comments of:

DONALD W. BURGESS[1] JAMES C. FANKHAUSER[3] LESLIE R. LEMON[5]
DUANE S. COOLEY[2] JOSEPH G. GALWAY[4] RONALD E. RINEHART[3]

Additionally, many useful comments were received from National Weather Service field employees.

The experience of working with National Weather Service Training Center students over the past five years has given me the unique opportunity to learn from almost 500 operational weather people. When it comes to weather, and probably a good many other things, *"Nobody Does It Better"* than the men and women of the National Weather Service!

Much of the material in this publication is a reorganization of a noteguide written by Larry Burns as part of the National Weather Service Training Center's radar course.

Thanks also to Dr. Richard Myers, Director of the Training Center, for creating an environment of academic freedom.

Finally, without the love and encouragement of Suzie, my partner over the past 22 years, this attempt would never have been made.

Robert Grebe
March 1982

Affiliations

1. National Severe Storms Laboratory
2. National Weather Service Headquarters
3. National Center for Atmospheric Research
4. National Severe Storms Forecast Center
5. Sperry Gyroscope - a division of
   Sperry Corporation

TABLE OF CONTENTS

AN OUTLINE OF SEVERE LOCAL STORMS WITH THE MORPHOLOGY OF ASSOCIATED RADAR ECHOES AND BIBLIOGRAPHY

R. Grebe

1. THUNDERSTORMS

1.1 Introduction

Right now, there are about 1000 thunderstorms in progress over the surface of the earth. Very few of these thunderstorms will be classified as severe (i.e., producing tornadoes, damaging surface winds or dime- to softball-sized hail). Of all the thunderstorms that occur in the Great Plains each year only one percent are severe. Most of the thunderstorms you experience will be relatively benign.

1.2 Thunderstorm Definition

In general, a local storm invariably produced by a cumulonimbus cloud, and always accompanied by lightning and thunder.

1.3 Climatology

It is useful to know where and when thunderstorms are likely to occur.

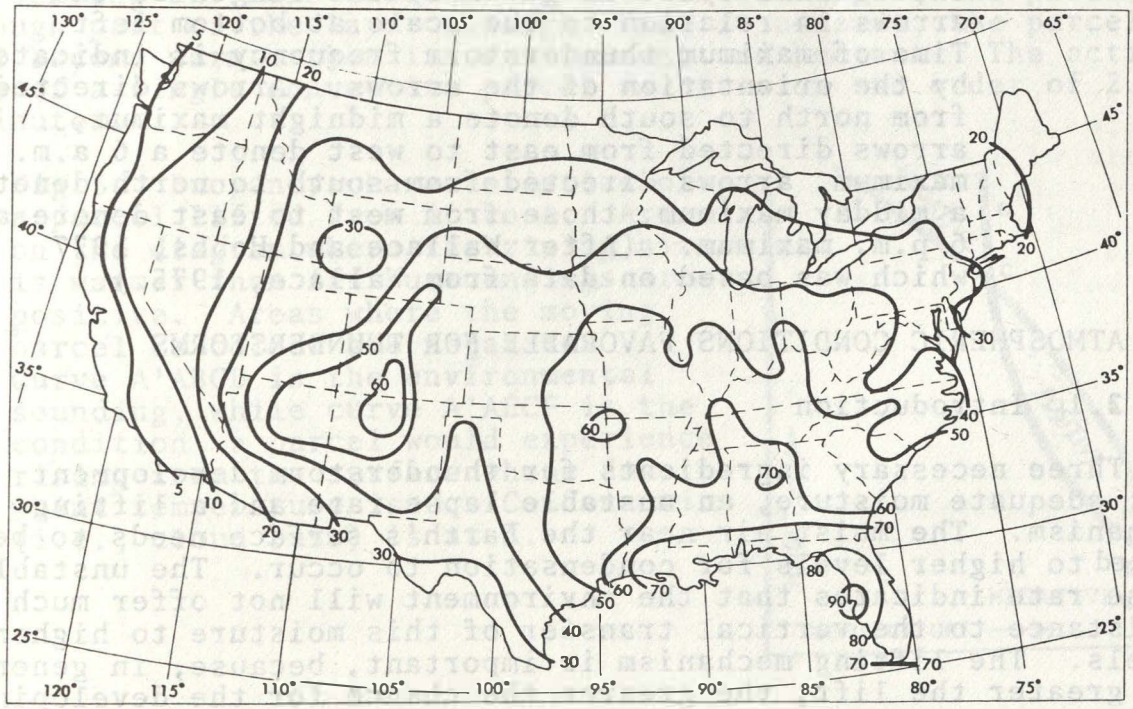

Fig.1. The geographic distribution of thunderstorms in the contiguous United States. Numbers represent the average number of days per year at any point over a 40-year period. (After Hydrometeorological Report No.5, Department of Commerce)

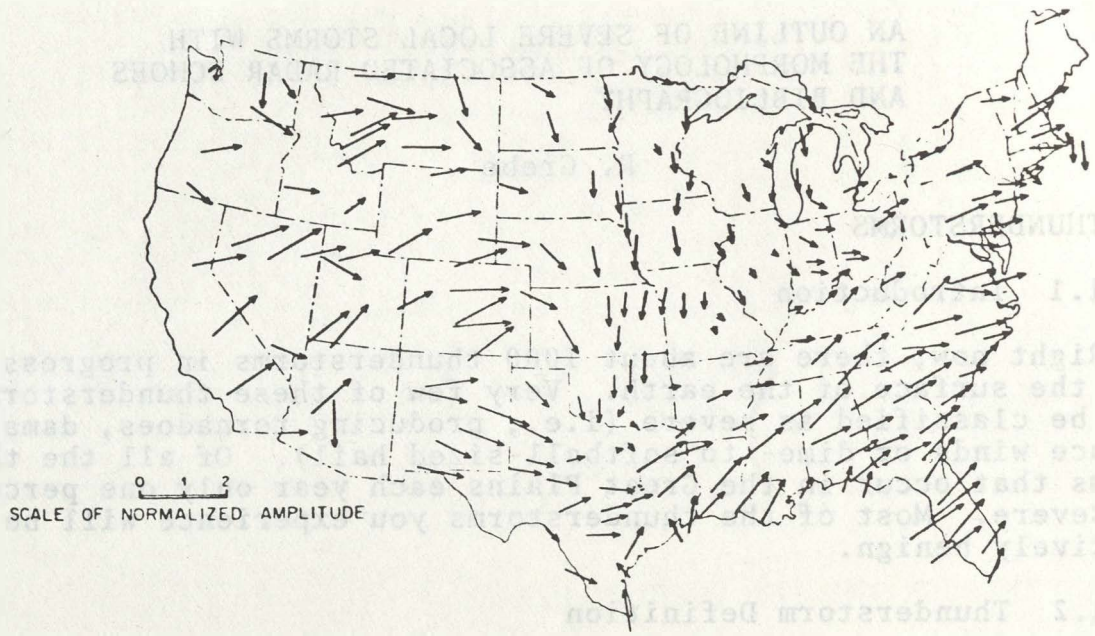

Fig.2. Diurnal variation of hourly thunderstorm frequency over the contiguous United States during summer (June-August). Normalized amplitude (division by the mean hourly thunderstorm frequency averaged over the 24 hours of the day at each station) of the diurnal cycle is given by the length of the arrows in relation to the scale at bottom left. Time of maximum thunderstorm frequency is indicated by the orientation of the arrows. Arrows directed from north to south denote a midnight maximum, arrows directed from east to west denote a 6 a.m. maximum, arrows directed from south to north denote a midday maximum, those from west to east denote a 6 p.m. maximum. (After Wallace and Hobbs, 1977 which was based on data from Wallace, 1975.)

2. ATMOSPHERIC CONDITIONS FAVORABLE FOR THUNDERSTORMS

2.1 Introduction

Three necessary ingredients for thunderstorm development are: adequate moisture, an unstable lapse rate and a lifting mechanism. The moist air near the Earth's surface needs to be lifted to higher levels for condensation to occur. The unstable lapse rate indicates that the environment will not offer much resistance to the vertical transfer of this moisture to higher levels. The lifting mechanism is important, because, in general, the greater the lift, the greater the chance for the developing thunderstorm to become severe.

The vertical transport and mixing of air is termed convection. We will consider the parcel, entrainment, and bubble theories of convection. Each theory has its good and bad points. The parcel

theory (Normand, 1946) is the simplest, but does not allow for mixing with the environment as the parcel rises. The entrainment theory (Stommel, 1947) is more realistic near smooth thunderstorm bases. The bubble theory (Scorer and Ludlam, 1953) predicts what our eyes observe when we look at the cauliflower tops of developing cumulonimbus clouds.

2.2 Adequate Moisture Content

The amount of moisture necessary to initiate thunderstorm development is variable. Thunderstorms do occasionally occur with surface temperatures and dewpoints below freezing; however, in general, the warmer and moister the air is in the lower 1.5 km (4920 ft), the greater the potential for thunderstorm development.

2.3 Unstable Lapse Rate

The rate of decrease of temperature with altitude is known as lapse rate. A body is said to be unstable if, after a small displacement, it tends to continue moving away from its original position.

2.4 Convection Theories

2.4.1 Parcel

An element of air is considered to rise without exchanging heat or water with its surroundings. If the lapse rate of the surrounding air mass exceeds the rate of cooling of the parcel through part of the layer through which it ascends, the parcel will become warmer than its environment and buoyant. The active life of a single convective parcel is often on the order of 2 to 5 minutes.

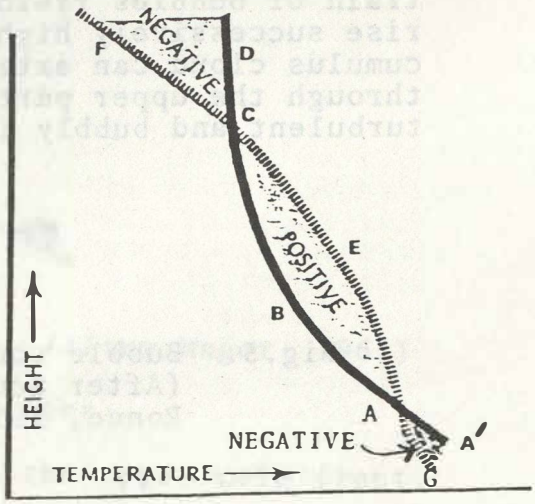

Fig.3. Buoyancy characteristics of a parcel lifted from A' to A. Areas on the diagram where the rising air is warmer than its surroundings are positive. Areas where the moving parcel is colder are negative. Curve A'ABCD is the environmental sounding, while curve A'AECF is the condition a parcel would experience rising from the surface whose dew point temperature is G. Condensation (i.e., cloud base) is at A.

In figure 3, some lifting force is required to move the parcel from A' to A. Once the parcel reaches A, it will rise along the path AEC because it is warmer than its surroundings. The parcel becomes colder than its surroundings at point C, but will continue to rise for awhile because of its momentum.

2.4.2 Entrainment

Vertical jets entrain (i.e., drag) air mostly along their edges, retaining a core of undiluted air that carries with it heat and water properties acquired near the Earth's surface. Aircraft flights near the bases of thunderstorms indicate that many updrafts are smooth and uniform in speed and thermal structure.

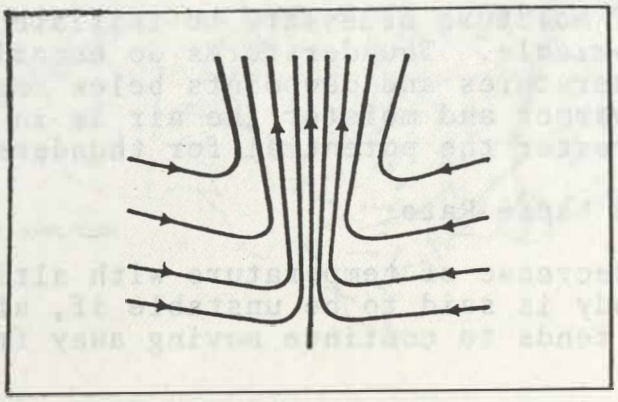

Fig.4. Vertical entraining convective jet. (After Stommel, 1947)

2.4.3 Bubble

Convection becomes organized into irregularly shaped cells in which air ascends in the interior of cells and descends at the common boundaries between the cells. The resulting updrafts have diameters ranging from 300-2,000 m (980-6,600 ft). On its own, an isolated bubble in an unsaturated environment can rise only a limited distance. In a train of bubbles rising through the same channel, each can rise successively higher before suffering erosion, and the cumulus cloud can extend to great heights. Aircraft flights through the upper parts of thunderstorms suggest they are turbulent and bubbly in appearance.

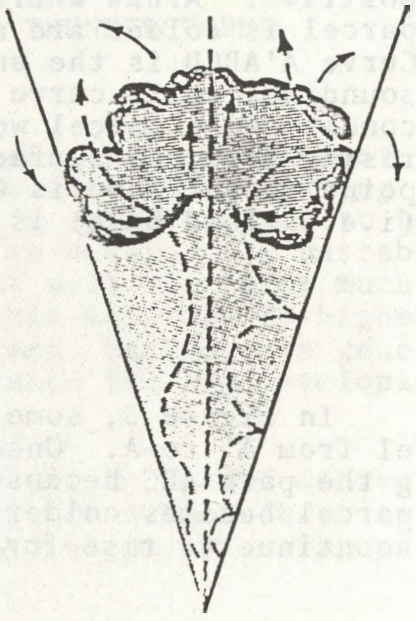

Fig.5. Bubble convection. (After Scorer and Ronne, 1956)

2.5 Lifting

Lifting is the forced upward motion that creates the initial updraft. Some lifting mechanisms are:

2.5.1 Convergence

If mass convergence is taking place in a layer near the surface of the Earth, the incoming air must be rising at the convergence line. This causes vertical motion and reduced stability. Surface convergence can be directional, where the wind changes direction towards a convergence line or speed, where the wind is linear and decreases in speed downwind along a convergence line perpendicular to the flow.

2.5.1.1 Boundary Convergence

The term boundary is used to denote a line along which there is a discontinuity between properties on either side of the line. Boundaries that are likely to provide significant updrafts include:

2.5.1.1.1 Cold Fronts

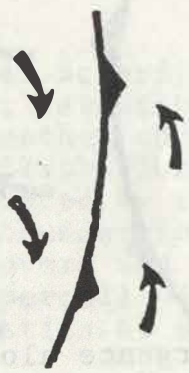

Fig.6. Convergence along a cold front. (After Magor, 1967)

2.5.1.1.2 Warm Fronts

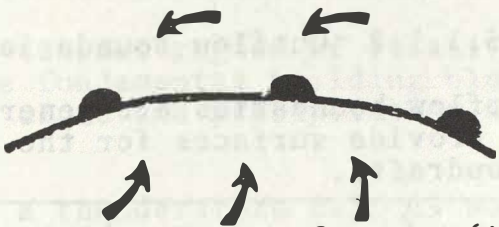

Fig.7. Convergence along a warm front. (After Magor, 1967)

2.5.1.1.3 Warm Front Occlusions

Increased lift occurs along the upper cold front.

2.5.1.1.4 Dry Lines

A dry line (i.e., dewpoint front) is defined as the discontinuity, indicated by a large dewpoint gradient, from moist to dry air at the surface. Dry lines exist primarily

through the western Plains and mark the boundary between continential tropical air on the west and maritime tropical air on the east.

2.5.1.1.5 Trough Lines

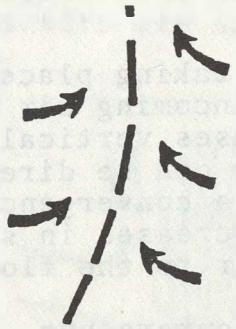

Fig.8. Convergence along a trough line. (After Magor, 1967)

2.5.1.1.6 Instability Lines

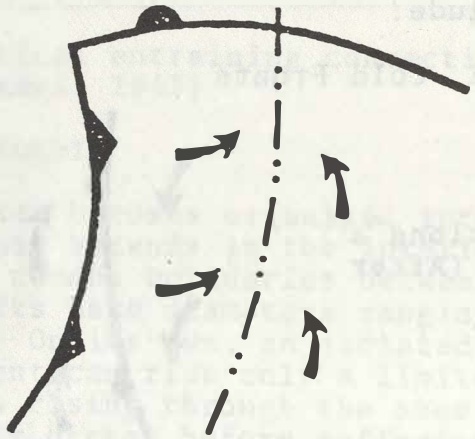

Fig.9. Convergence along an instability line. (After Magor, 1967)

2.5.1.1.7 Outflow Boundaries

Outflow boundaries are generated by thunderstorm downdrafts and can provide surfaces for the maintenance or initiation of new updrafts.

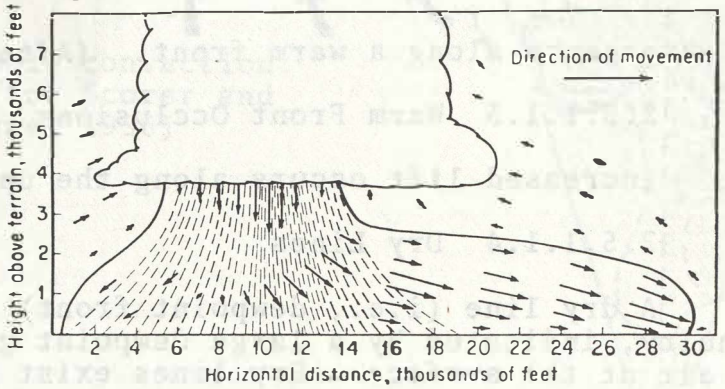

Fig.10. Vertical cross section through a cold dome of outflowing downdraft air. (After Byers, 1974)

2.5.2 Orographic

Thunderstorms are formed when wind blowing over rising ground causes lifting of the air and increased instability. In general, the higher the terrain obstruction, the greater the lift.

2.5.3 Surface Heating

Thunderstorm updrafts over land tend to develop in the afternoon. Their development is usually explained as a result of surface heating due to solar radiation. They are often referred to as air mass thunderstorms. Solar radiation also aids in thunderstorm development when dynamic lifting occurs.

Thunderstorm updrafts over water tend to develop before dawn in the absence of dynamic lifting. This is usually explained in terms of the water surface being warmer than the land during the early morning hours. Instability is further increased as the top of the cloud loses heat by radiation to outer space.

3. THE ORDINARY THUNDERSTORM

3.1 Introduction

Thunderstorms are usually classified according to the physical processes immediately involved in their formation, e.g., orographic, frontal, heat, etc. The operational weather community is concerned with thunderstorm severity and flash flood potential. This outline utilizes modeling concepts advanced by the research community during the 1970's and classifies thunderstorms as nonsevere (i.e., the ordinary thunderstorm) or severe and lists characteristics of each model. In theory, a supercell severe thunderstorm in New England has the same characteristics as one in England.

3.2 Difference Between Thunderstorm Cells And Radar Cells

Cells represent a compact region of relatively strong vertical air motion and are the fundamental building blocks of thunderstorms. The updraft generates cloud and precipitation while the downdraft evaporates same.

The definition of a thunderstorm cell is not the same as a radar cell. A radar cell usually represents a compact cluster of environmental cells that appear on the plan position indicator as a single cell with a nucleus of higher reflectivity.

3.3 Rainshower Or Thundershower?

A common rule-of-thumb states that echo tops of 7.6 km (25 kft) or greater usually indicate thunder. This rule works best at 35° north latitude. To adjust for your latitude, subtract 2000 ft for every 1° north of 35°N or add 2000 ft for every 1° south of 35°N. Unrealistic results will be obtained for locations like Bangor, Maine, or Miami, Florida. The rule is approximate and, in general, echo tops associated with thunder tend to be lower the more northerly the latitude and tend to be higher the more southerly the latitude.

Kotov (1960) in a study of thundershowers in northern Russia found that 93% of the tops of echoes associated with thundershowers penetrated the -22°C isotherm aloft.

3.4 Evolution

Warm moist air near the Earth rises and replaces denser air aloft. The lifting results in the condensation of atmospheric water vapor forming a visible cloud of water droplets. The release of heat (i.e., latent heat of condensation) acts to speed the overturn (i.e., drive the updrafts). A weak-to-moderate updraft is often forced to lean downstream by the surrounding wind field. Precipitation particles forming in the updraft fall out as they grow. Cooling caused by the evaporation of condensed water helps drive the downdrafts, which replace some of the subcloud air. New cells frequently occur on the flanks of old cells in response to low-level convergence created by the gust front. (See "gust front" section on page 35.) Thunderstorms range from 3-50 km (2-31 mi) in the horizontal and may extend hundreds of kilometers in squall lines. An individual thunderstorm typically covers a surface area of 500-2500 km^2 (200-1000 mi^2) and may consist of one or more distinct cells, each of which is several miles across. Total lifetime varies from 1/2 to 1 hour for the single cell ordinary thunderstorm to less than 1 1/2 hours for the weaker ordinary multicellular thunderstorms. Thunderstorms typically travel at speeds from near zero to 27 m/s (60 m/h) and occasionally exceed 45 m/s (101 m/h).

3.4.1 Cumulus Stage

Cells consist primarily of updrafts with precipitation suspended aloft. The cumulus stage lasts about 15 minutes.

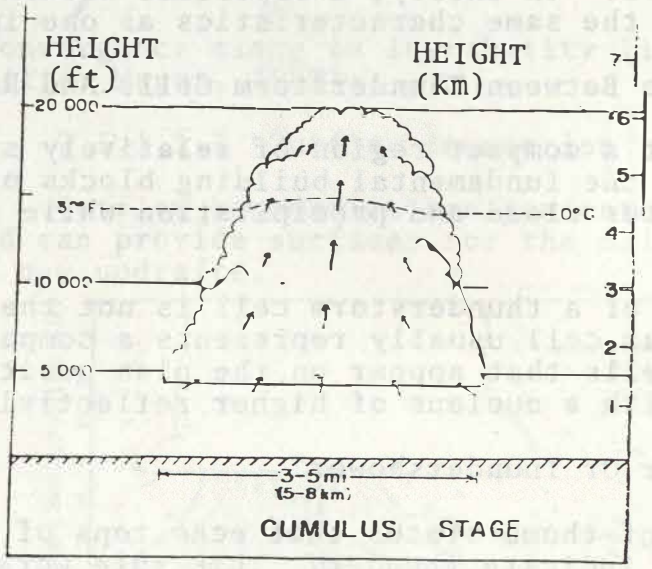

Fig.11. Cumulus stage. (Diagram by C. Doswell)

3.4.2 Mature Stage

Updrafts and downdrafts 15 m/s (34 m/h) or greater coexist side by side. Precipitation descending to the surface creates a downdraft originating from the midlevel environment

where dryer air is entrained and evaporated. The strongest downdrafts are found in the lower part of the cloud and produce a diverging pool of cool air with the leading edge forming a micro-cold front (i.e., gust front). New cells tend to form above this outflow. Heavy rain falls to the ground and hail, if any, occurs. Most tops reach 9-18 km (30-59 kft) above the ground. The upper part of the cloud glaciates and spreads laterally due to the continued updraft and divergence aloft.

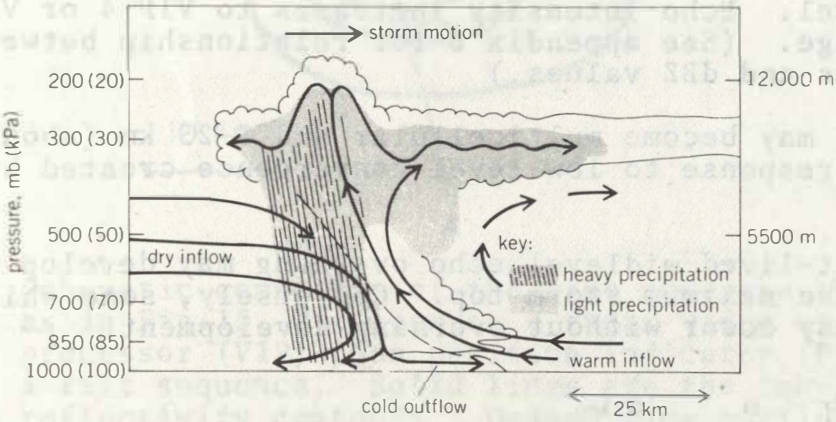

Fig.12. Cloud boundaries and simplified circulation (arrows denote flow) of a typical mature thunderstorm in winds which blow from left to right and increase with height. Vertical scale has been exaggerated fivefold compared with the horizontal scale. (After Davies-Jones, 1980)

3.4.3 Dissipating Stage

The downdraft spreads through the entire cell, weakens and disappears. Only light precipitation occurs and generally is not prolonged.

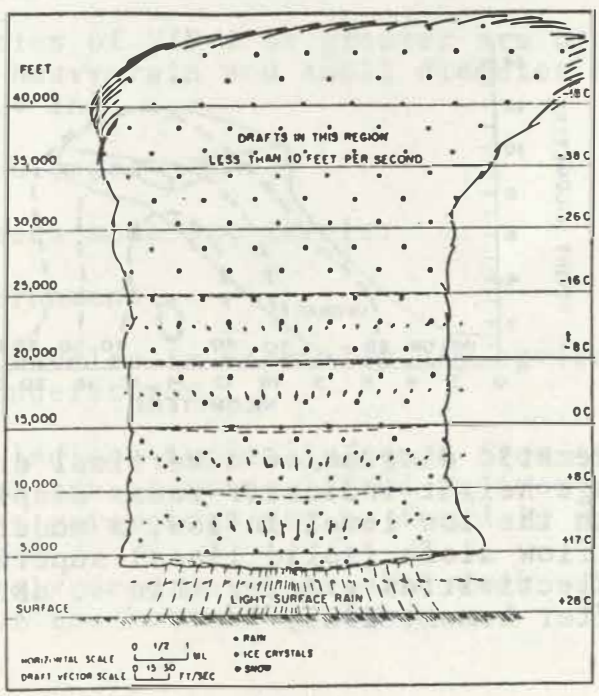

Fig.13. Dissipating stage. (After Byers and Braham, 1949)

3.5 Radar Model

The storm top, midlevel, and low-level reflectivity cores are generally aligned one below the other. (See appendix A for height ranges of low, mid and upper levels.) The storm may even tilt downwind with height in environments with strong mid- and high-level winds.

The first echo develops aloft from 3-6 km (10-20 kft) above ground level. Echo intensity increases to VIP 4 or VIP 5 in the mature stage. (See appendix B for relationship between VIP intensities and dBZ values.)

Echoes may become multicellular and 5-25 km (about 3-14 nmi) across in response to low-level convergence created by the gust front.

A short-lived midlevel echo overhang may develop without a shift in the maximum storm top. Conversely, some shift in the echo top may occur without overhang development.

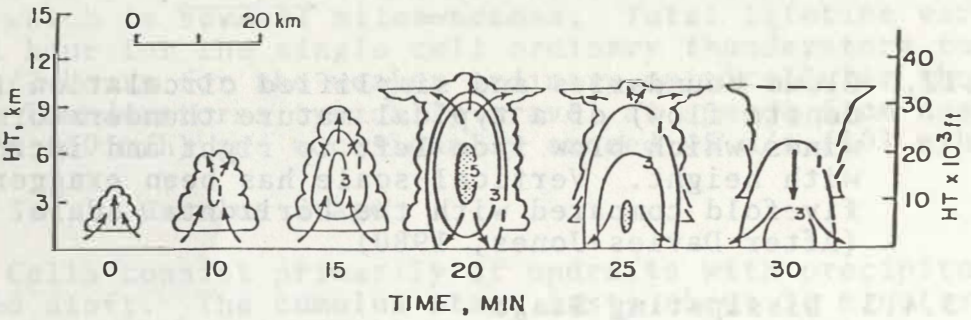

Fig.14. The ordinary thunderstorm developing in an unstable airmass, with daytime heating of the Earth's surface. Contours are in 10's of dBZ. (After Wilk, et al., 1978 adapted from Chisholm and Renick, 1972)

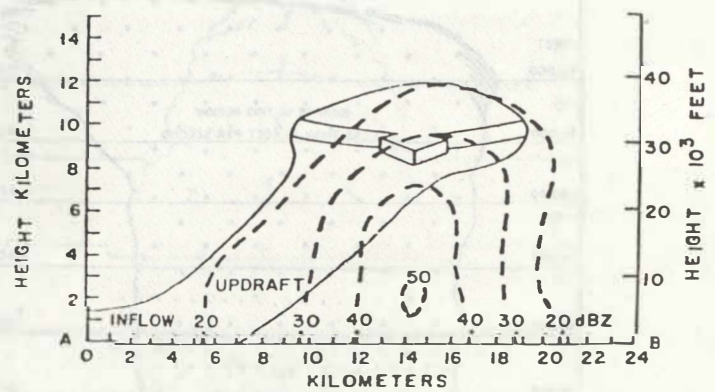

Fig.15. Schematic diagram of a vertical cross-section or range height indicator radar display of a thunderstorm with the low-level inflow, a moderate updraft, and outflow aloft (solid lines) superimposed. Radar reflectivities greater than 50 dBZ (VIP 5) stippled. (After Lemon, 1980)

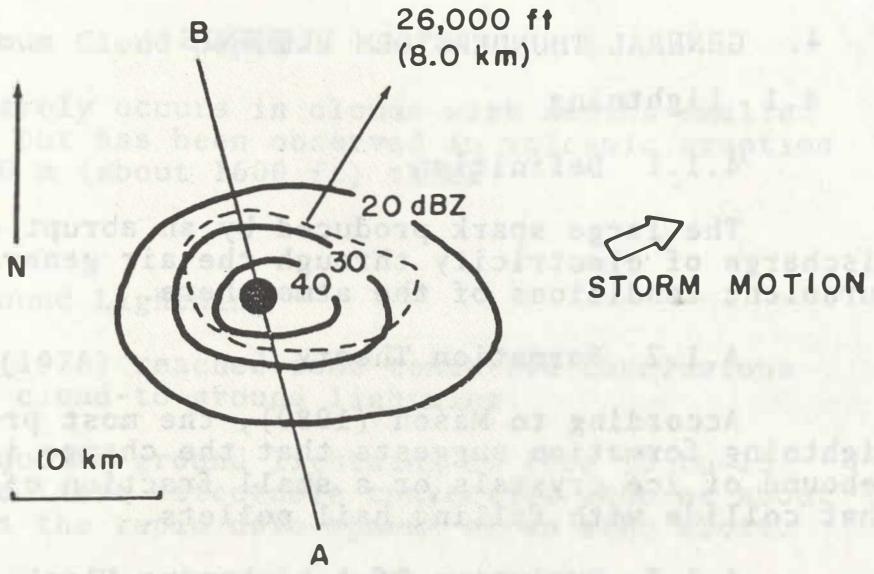

Fig.16. Schematic composite of the same moderate thunderstorm as in Fig.15, but seen on a radar video integrator processor (VIP) plan position indicator (PPI) during a tilt sequence. Solid lines are the low-level reflectivity contours. Dashed line outlines the echo greater than or equal to 20 dBZ (VIP 1) derived from the midlevel elevation scan. The black dot is the location of the maximum echo top from the high-level scan. (After Lemon, 1980)

3.6 Characteristics

3.6.1 Severe Weather

None. However, cloud to ground lightning is possible in all thunderstorms.

3.6.2 Hydrometeors

Reflectivities of VIP 4 or greater are usually found to be associated with heavy rain and small diameter hail, less than or equal to 1 cm (.4 in).

3.6.3 Turbulence

Rarely exceeds moderate levels.

3.6.4 Environment

A. Storms develop in virtually any environment favorable for thunderstorms.

B. Lifted indices typically range from +4 to -4. (Information on using lifted indices as thunderstorm forecast parameters can by found in appendix C.)

C. Relatively deep moisture with weak vertical wind shear of the horizontal winds.

4. GENERAL THUNDERSTORM ELEMENTS

4.1 Lightning

4.1.1 Definition

The large spark produced by an abrupt discontinuous discharge of electricity through the air generally under turbulent conditions of the atmosphere.

4.1.2 Formation Theory

According to Mason (1980), the most promising theory of lightning formation suggests that the charge is produced by the rebound of ice crystals or a small fraction of the cloud droplets that collide with falling hail pellets.

4.1.3 Evolution Of A Lightning Flash

Battan (1980) describes the evolution of a lightning flash as a series of step leaders and return strokes. A surge of electrons moves downward a short distance for about one millionth of a second and then stops. After pausing, another step takes place. The sequence is repeated until the leader reaches the ground. The charge then moves rapidly up the path taken by the step leader, i.e., return stroke. After one hundredth of a second another stroke occurs in the same channel. As many as 30-40 strokes have been observed in this channel.

4.1.4 Probable Charge Distribution

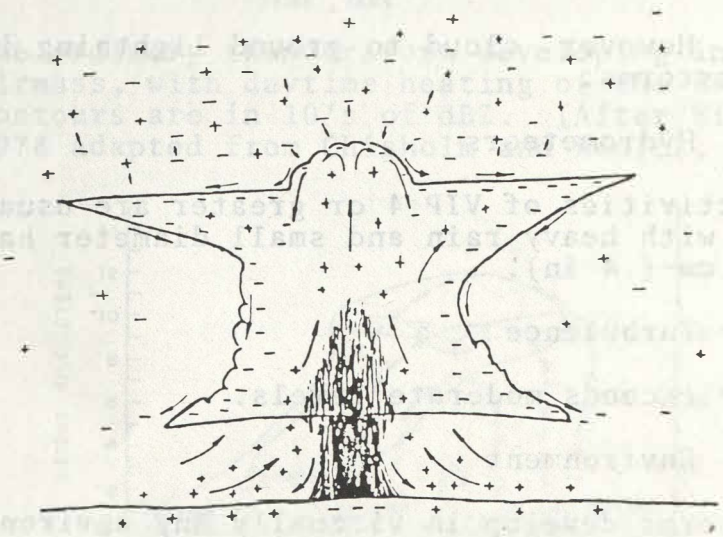

Fig.17. A schematic view of the probable distribution of charges in and around a thundercloud. (After Moore and Vonnegut, 1977)

4.1.5 Relationship Of Lightning To Updrafts

In a thunderstorm cell the main electrical activity starts only in the most active updraft region.

4.1.6 Minimum Cloud Depth

Lightning rarely occurs in clouds with depths smaller than 3 km (10 kft), but has been observed in volcanic eruption clouds less than 500 m (about 1600 ft) thick.

4.1.7

Cloud-To-Ground Lightning

Fitzgerald (1978) reached some tentative conclusions about the nature of cloud-to-ground lightning:

1. The onset of cloud-to-ground lightning is from 10 to 15 minutes from the first detectable convective echo or about the same time as the rapid development of an echo aloft.

2. Rapid echo growth is in the -10°C to -20°C temperature region aloft and is closely related to the development of charge concentration.

3. Cloud-to-ground lightning is most often found within 2 miles of echo cores seen at low elevation angles.

4. Probability of cloud-to-ground lightning

TEMPERATURE OF TOPS	VIP	PERCENT (CUMULATIVE)
-10°C to -20°C	1	10%
-30°C	2&3	70%
-40°C	5	100%

Kinzer (1972) established a relationship between storm intensity and cloud-to-ground lightning. The suggestion is that areas of stronger reflectivity may have higher rates of cloud-to-ground lightning.

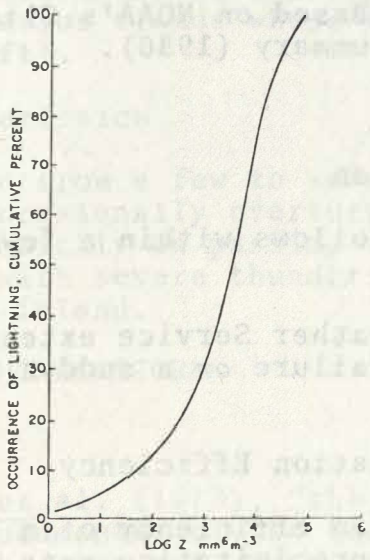

Fig.18. Storm intensity and the occurrence of cloud-to-ground lightning. (After Kinzer, 1972)

4.1.8 Danger To People

Over the years more people are killed by lightning than tornadoes, hurricanes, or flash floods.

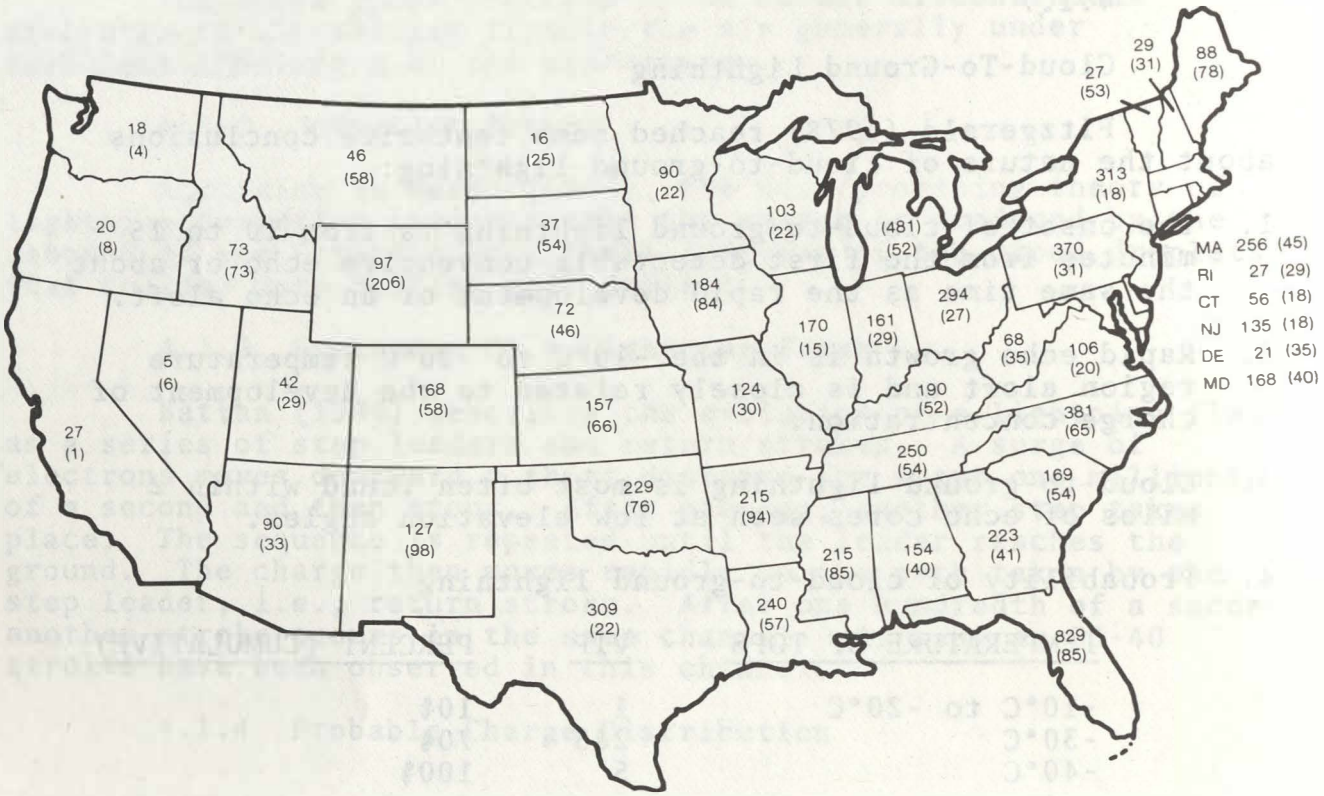

Fig.19. Frequency of lightning deaths and injuries 1959-1980. (Approximate number of hits per million people). Based on NOAA's Climatological Data, National Summary (1980).

4.2 Flash Floods

4.2.1 Definition

A flood which follows within a few hours of heavy or excessive rainfall.

The National Weather Service extends this definition to include a dam or levee failure *or* a sudden release of water impounded by an ice jam.

4.2.2 Precipitation Efficiency

The precipitation efficiency of a thunderstorm is defined as the ratio of surface precipitation rate to water vapor input.

Browning (1977) found the precipitation efficiency of thunderstorms to range from 2-100%. Newton (1968) found that about 40-45% of the water vapor entering the cloud falls to earth as precipitation in midwestern thunderstorms.

4.2.2.1 Relationship Between Severe Local Storms And Flash Flooding

Browning (1977) states that studies have shown an inverse relationship between the precipitation efficiency and the environmental wind shear in the cloud-bearing layer. The *least* efficient storms tend to be supercell hailstorms. Highly efficient rainstorms tend not to produce hail.

Maddox et al. (1979) found that flash flooding occurred either before, during, or after an associated severe weather event in about 50% of 151 flash flood cases.

4.3 Hail

A discussion of hail is included in the "severe local storm elements" section beginning on page 30.

4.4 Waterspouts

4.4.1 Definition

An intense whirling, funnel-shaped vortex, extending from a cumulus-type cloud down several hundred to several thousand feet to the water surface.

4.4.2 Visible Structure And Evolution

The visible funnel consists mostly of atmospheric water vapor condensed because of lower pressure in the vortex. Water or spray salt drawn from the underlying surface also contributes to the structure and visibility of the funnel. Most waterspouts are associated with cumulus clouds whose tops may not extend above 6 km (about 20 kft).

4.4.3 Characteristics

Diameters range from a few to several hundred feet. Waterspout winds can occasionally overturn small vessels. Most waterspouts dissipate quickly on passing inland; however, a small number are associated with severe thunderstorms and become tornadoes as they move inland.

5. THE PULSE SEVERE THUNDERSTORM

5.1 Introduction

According to Wilk et al. (1978), "the pulse severe thunderstorm is perhaps the least documented of the thunderstorm models. However, it does appear to be the simplest, most easily identifiable, and one of the shortest lived." This model is sometimes referred to

as the Alberta Hailstorm (Chisholm, 1973).

5.2 Evolution

This storm closely resembles the ordinary thunderstorm and is frequently multicellular. Updrafts are short lived, in the form of a bubble or pulse, with suspected vertical velocities of near 30 m/s (67 mi/h) or more. Total storm lifetime is 1 to 2 hours.

5.3 Radar Model

The first detectable echo is from 7-9 km (23-30 kft) AGL.

A VIP 5 (50 dBZ) echo core develops higher than in an ordinary thunderstorm and maintains continuity with descent to the ground.

A VIP 5 echo detected at or above 9 km (30 kft) increases the probability of storm severity.

Hook echoes are rare!

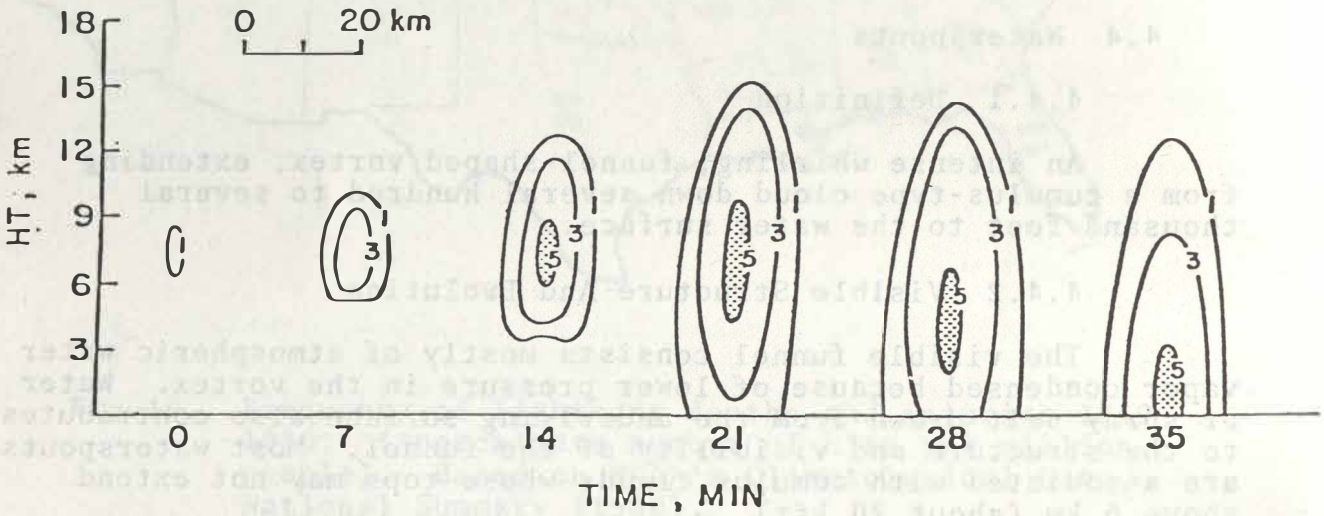

Fig.20. Range height indicator profile of a pulse severe thunderstorm. Reflectivity values are in tens of dBZ. (After Wilk, et al., 1978)

5.4 Characteristics

5.4.1 Severe Weather

A. Hail to 5 cm (2 in) has been associated with the VIP 5 area.

B. Damaging surface winds.

C. A few short-lived tornadoes are possible.

D. The period of severe weather may be only 12 to 17 minutes.

5.4.2. Hydrometeors

Large hail and high liquid water concentrations aloft.

5.4.3 Turbulence

Can be extreme.

5.4.4 Environment

A. Moderate to strong instability with lifted indices less than -3.

B. Weak vertical wind shear.

C. Most frequent during the summer months.

6. THE MULTICELL SEVERE THUNDERSTORM

6.1 Introduction

The multicell severe thunderstorm has been documented by Chisholm and Renick (1972), also by Wilk, Lemon and Burgess (1978). Nelson (1976), studying Oklahoma hailstorms, found the average maximum hail size was 1.9 cm (.75 in) and the average maximum width of the hail swath was 10 km (6 mi).

6.2 Evolution

New cells tend to develop on the right or right rear storm flank, with two to four cells existing at any one time during the life of the storm. Cell development occurs every 5 to 10 minutes, resulting in a midlevel echo overhang with a weak echo region (WER) beneath. All overhang does not indicate updraft, but persistent overhang along the echo flanks is believed to reflect rising air within the storm's weak echo region.

6.3 Radar Model

In general, the stronger the storm's updraft, the greater the potential for severity. The weak echo region of the multicell severe thunderstorm and the bounded weak echo region of the supercell severe thunderstorm are usually associated with strong updrafts. Evidence suggests that the hydrometeors do not have time to grow to large size in a strong updraft, and thus are not, or only weakly, detected by radar. Conversely, Nelson (1977) has documented a weak echo region due to evaporation of falling precipitation in a developing downdraft.

When the low-level echo core and storm top shift towards the updraft flank (i.e., edge of strongest low-level reflectivity gradient) the midlevel echo overhang projects out by 6-25 km (about 3-14 nmi) from the updraft flank and the echo slows and turns 15° to 100° to the right of the other nonsevere echoes. *The probability that severe weather is occurring at the surface or will begin in the next 30 minutes is now high.*

6.3.1

Radar Characteristics

A. Maximum storm tops frequently reach 12 km (about 39 kft) and have reached near 20 km (about 66 kft) AGL.

B. The storm appears in the low levels as a single large echo 15-40 km (about 9-25 mi) with two or more reflectivity cores and echo tops aloft.

C. Midlevel reflectivities exceed VIP 4 (45 dBZ).

D. Discrete propagation of new cells occurs on the right flank while old cells dissipate on the left flank.

E. Storm movement is usually to the right of and slower than other weaker, nearby storms but can be to the left of or identical to the mean winds.

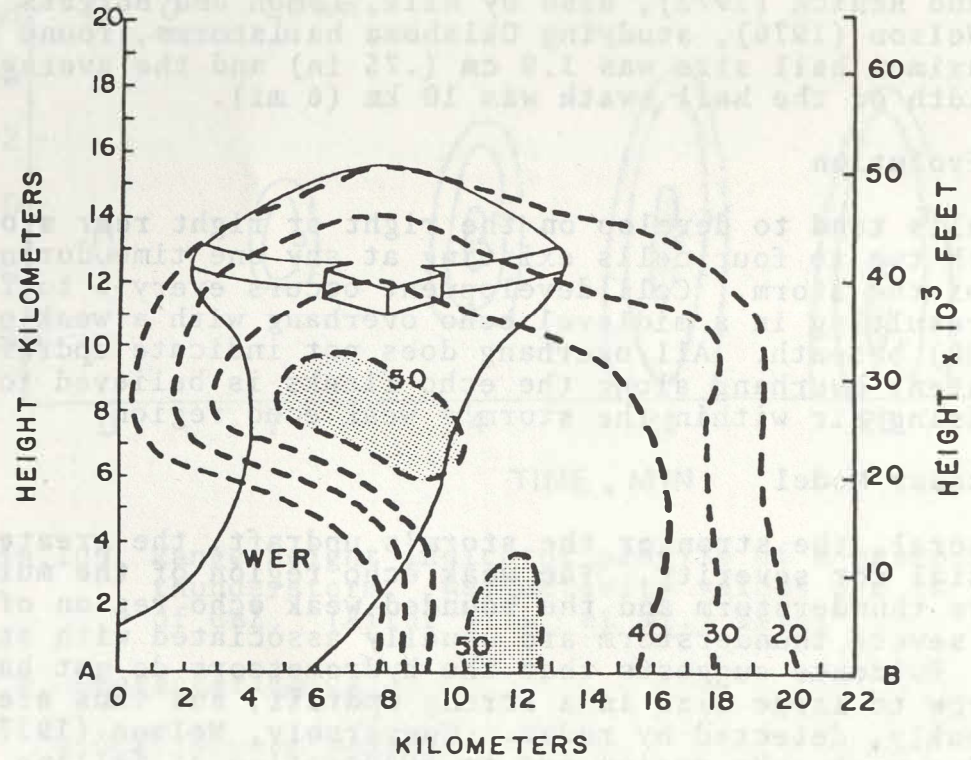

Fig.21. Vertical cross section depicting strong updraft and weak echo region. Legend same as Fig.15, page 10. (After Lemon, 1980)

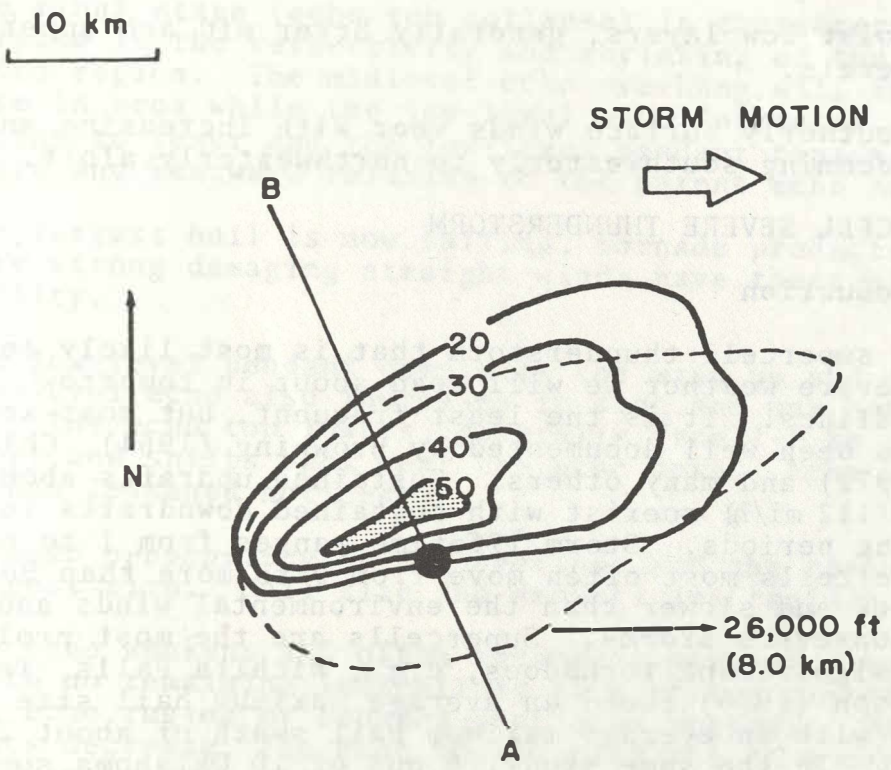

Fig.22. Low-level reflectivity depiction with line AB corresponding to line AB of Fig.21. Legend same as Fig.16, page 11. (After Lemon, 1980)

6.4 Characteristics

6.4.1 Severe Weather

A. Large hail.

B. Damaging winds.

C. Short-lived tornadoes.

6.4.2 Hydrometeors.

A. Hail reaches the ground first associated with strong low-level reflectivity gradients.

B. Heavy rain, smaller hail, and strong downdrafts are associated with the storm core as the cell matures.

6.4.3 Turbulence

Strong or severe turbulence is likely to be encountered along the south echo flank from the surface to upper levels during the most intense phase of each cell.

6.4.4 Environment

A. Moderate to strong instability (-3 to -12 lifted index).

B. Moist low layers, generally dryer mid and upper levels.

C. Southerly surface winds veer with increasing speed, becoming southwesterly to northwesterly aloft.

7. THE SUPERCELL SEVERE THUNDERSTORM

7.1 Introduction

It is the supercell thunderstorm that is most likely to produce the severe weather we will read about in tomorrow morning's headlines. It is the least frequent, but most severe. This storm has been well documented by Browning (1964), Chisholm and Renick (1972) and many others. Sustained updrafts about 25-50 m/s (56-112 mi/h) coexist with sustained downdrafts for relatively long periods. Storm lifetime ranges from 1 to 6 hours or more. Supercells most often move from 0 to more than 90° to the right of and slower than the environmental winds and neighboring nonsevere storms. Supercells are the most prolific producers of significant tornadoes, e.g., Wichita Falls, Texas, in 1979. Nelson (1976) found an average maximum hail size of 5.3 cm (2 in) with an average maximum hail swath of about 20 km (about 12 mi). In the same study, 6 out of 10 Oklahoma supercells produced funnel clouds or tornadoes.

7.2 Evolution

Lemon (1980) lists four distinct evolutionary stages of the supercell:

The first stage (nonsevere) often begins with a multicell storm (Fig.15, page 10, and Fig.16, page 11) that is isolated or in a scattered line. There is no midlevel echo overhang in this stage and the storm top is over the low-level reflectivity cores.

The second stage (severe hail storm) occurs as each cell in the series developing on the updraft flank of the storm becomes stronger as the storm develops into a severe multicell (Fig.21, page 18, and Fig. 22, page 19) or single cell storm. The midlevel echo increases rapidly in size and/or intensity, usually on the right flank of the low-level echo above and around the updraft, as the weak echo region develops. Surface hail is usually 2-6 cm (0.8-2.4 in).

The third stage (mature supercell) occurs when the storm acquires an intense updraft rising nearly vertically despite strong environmental winds. A radar-detected bounded weak echo region may develop and is capped above by strong reflectivities and, further aloft, by the storm top (Fig.23, page 21). The storm top may rise above 18 km (59 kft). The low-level echo is characterized by concavity, bordered by intense reflectivity gradients and bounded at the rear by a pendant or hook echo beneath the midlevel overhang as the right rear echo flank swings southward (Fig.24, page 22). Maximum surface hail usually equals or exceeds 4.5 cm (1 3/4 in), surface winds often exceed 25 m/s (56 mi/h), and funnel clouds or tornadoes occur.

The final stage (echo top collapse) is characterized by an increase in the reflectivity and shrinking of the bounded weak echo region. The midlevel echo overhang will frequently decrease in area while the low-level echo increases. The echo top begins to lower and the low-level pendant typically swings southward and eastward relative to the parent echo body.

The largest hail is now falling, tornado production begins, and very strong damaging straight winds have their highest probability.

The low-level pendant completes the wrap up and disappears. The low-level echo also increases in size and may begin to weaken. The echo top lowers, generally from 2-7 km (about 7-23 kft) and shifts back near the echo core. Echo overhang extent has lessened noticeably.

Tornado probability is now greatest and the tornado reaches its largest size. Hail size and amounts are rapidly decreasing.

The echo weakens and often becomes a part of a solid squall line with no remaining indications of a strong updraft (i.e., no weak echo region or bounded weak echo region). Reflectivity gradients decrease, the echo top is over the echo core, and the storm often becomes multicellular.

Tornadoes have now dissipated.

New updrafts, especially if the echo remains separated from other echoes, may cycle through this evolution with repeated severe weather and tornado production.

7.3 Radar Model

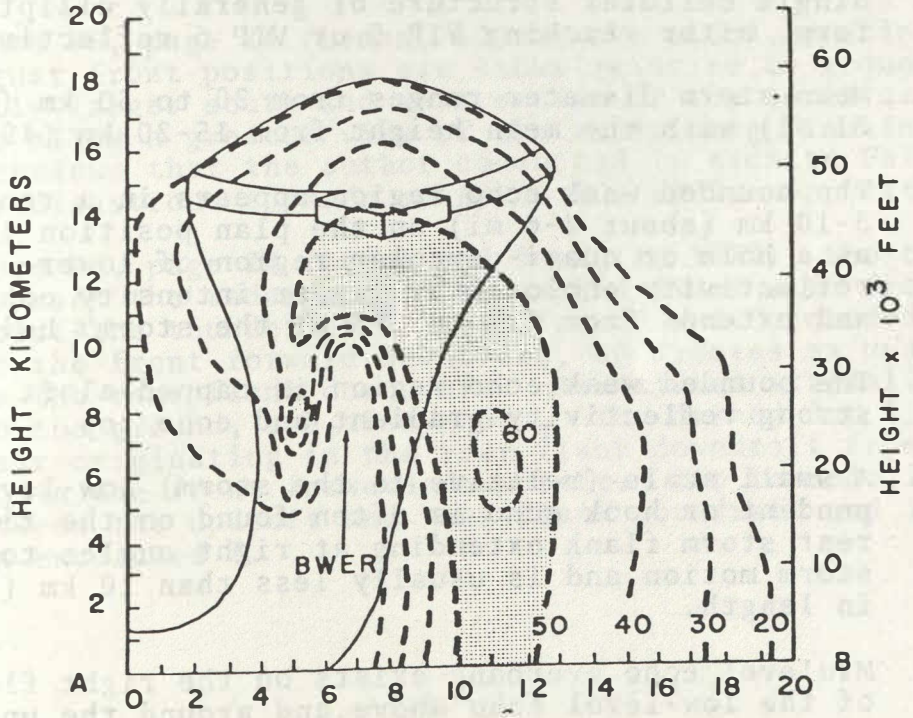

Fig.23. Vertical cross section of mature supercell. Legend same as Fig.15, page 10. (After Lemon, 1980)

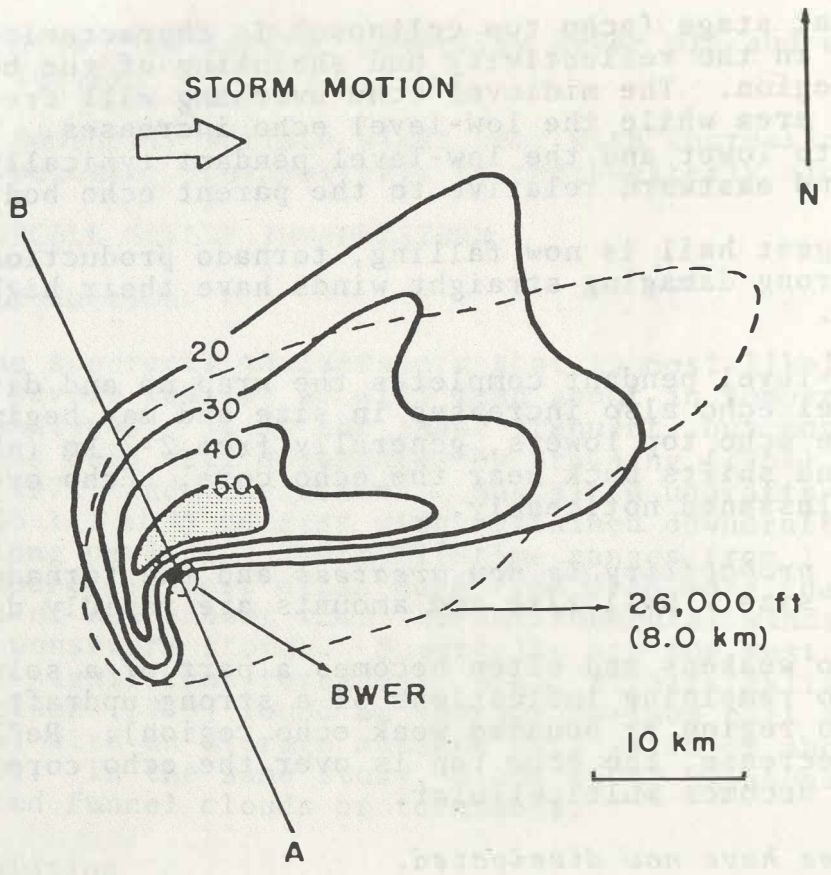

Fig.24. Low-level plan view of mature supercell. Legend same as Fig.16, page 11. (After Lemon, 1980)

7.3.1 Radar Characteristics

A. Single cellular structure of generally elliptical form, after reaching VIP 5 or VIP 6 reflectivity.

B. Mean storm diameter ranges from 20 to 50 km (12-31 mi) with the mean height from 15-20 km (49-66 kft).

C. The bounded weak echo region appears in a range from 3-10 km (about 2-6 mi) on the plan position indicator as a hole or quasi-circular region of lower reflectivity enclosed by higher intensity echoes and extends from 1/2 to 2/3 of the storm's height.

D. The bounded weak echo region is capped aloft by a strong reflectivity gradient and echo top.

E. A small scale (relative to the storm) low-level pendant or hook echo is often found on the right rear storm flank extending at right angles to storm motion and is usually less than 10 km (6 mi) in length.

F. Midlevel echo overhang exists on the right flank of the low-level echo above and around the updraft.

G. During the echo top collapse, the reflectivity of a shrinking bounded weak echo region increases, and the echo top shifts over the low-level echo core. The areal extent of the echo at midlevels will decrease..

7.4 Characteristics

7.4.1 Severe Weather

The extremes of tornadoes, downbursts, and giant hail.

7.4.2 Hydrometeors

Giant hail in the high reflectivity gradients enclosing the bounded weak echo region. Smaller hail and very heavy rain associated with the low-level reflectivity core of the storm.

7.4.3 Turbulence

Extreme!

7.4.4 Environment

A. Strongly sheared with strong low-level southerly flow veering to southwest or west aloft.

B. Low levels are moist and very unstable with dry air in mid to upper levels.

7.5 Surface Weather And Storm Structure Of A Supercell

Research during the 1970's produced a supercell storm model that is useful in anticipating surface severe weather occurrence.

In figure 25, page 24 (Lemon, 1979), the cloud, precipitation areas and gust front positions are shown relative to ground level. The typically larger south and west extent of the anvil canopy is lessened to allow a greater view of the underlying flanking line. Public interviews that the author conducted in Wichita Falls, Texas, after their disastrous tornado of April 10, 1979, supported this model.

In figure 26, page 24 (Lemon and Doswell, 1979), the thickest line encompasses the radar echo. The solid lines with frontal symbols depict the thunderstorm "gust front" and "occluded wave". FFD denotes the front forward downdraft, UD denotes an updraft and RFD denotes the rear flank downdraft. Associated streamlines, relative to the ground, are also shown. The dashed dot line separates air originating in the rear flank downdraft from that originating in the front forward downdraft. The tornado is located between the updraft and rear flank downdraft and is shown by an encircled T.

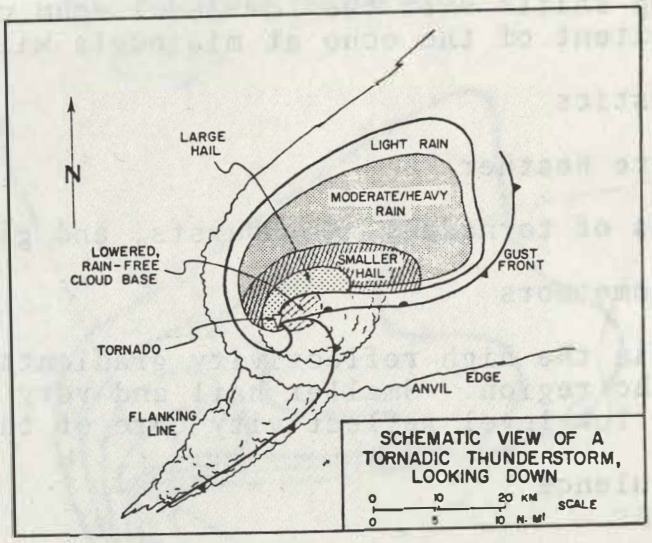

Fig.25. Schematic view of a tornadic thunderstorm. (After Lemon, 1979)

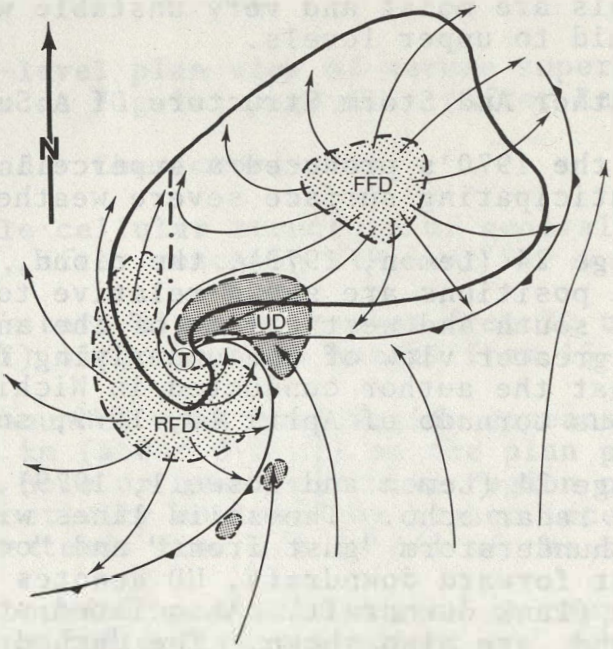

Fig.26. Schematic plan view of a supercell thunderstorm at the surface. (After Lemon and Doswell, 1979)

8. SEVERE LOCAL STORM ELEMENTS

8.1 The Tornado

Tornadoes are the most violent storms on earth with estimated wind speeds up to 134 m/s (300 mi/h). The spinning motion of a tornado is almost always counterclockwise. The words twister and cyclone are sometimes used as tornado synonyms. The expression "tornado on the ground" is technically redundant because the definition of a tornado implies contact with the ground.

8.1.1 Definition

A violently rotating narrow column of air in contact with the ground and extending from a thunderstorm base.

8.1.2 Difference Between A Tornado And A Funnel Cloud

A funnel cloud is a funnel-shaped cloud extending from a towering cumulus or cumulonimbus base associated with a rotating air column that is *not* in contact with the ground. Once the rotating air column comes in contact with the ground, it becomes, by definition, a tornado.

8.1.3 Formation And Visual Structure

In figure 27, page 26, the wall cloud appears as a lowered rain-free cloud base from 1.6-6.5 km (1-4 mi) in diameter, usually situated in the southwest part of the storm, below an intense updraft. Tornadoes are often located beneath the right or rear periphery of the wall cloud. A rotating wall cloud usually develops a few minutes to possibly an hour before tornadoes or funnel clouds.

A clear slot often originates to the rear and right rear of the tornado resulting from the rear flank downdraft (RFD in figure 26, page 24. Burgess et al. (1977) found the clear slot to be associated with a radar-indicated downdraft and hook echo.

Newton (1980) explains the visible funnel or tornado as resulting from the condensation of cloud droplets. The droplets condense because of markedly (100-200 mb) lower pressure in the vortex than in the surroundings. The intense winds result from the inward-moving rings of air increasing in rotary motion under the conservation of angular momentum. Air rises up to 67 m/s (150 mi/h) in the sheath of the funnel and descends near its core.

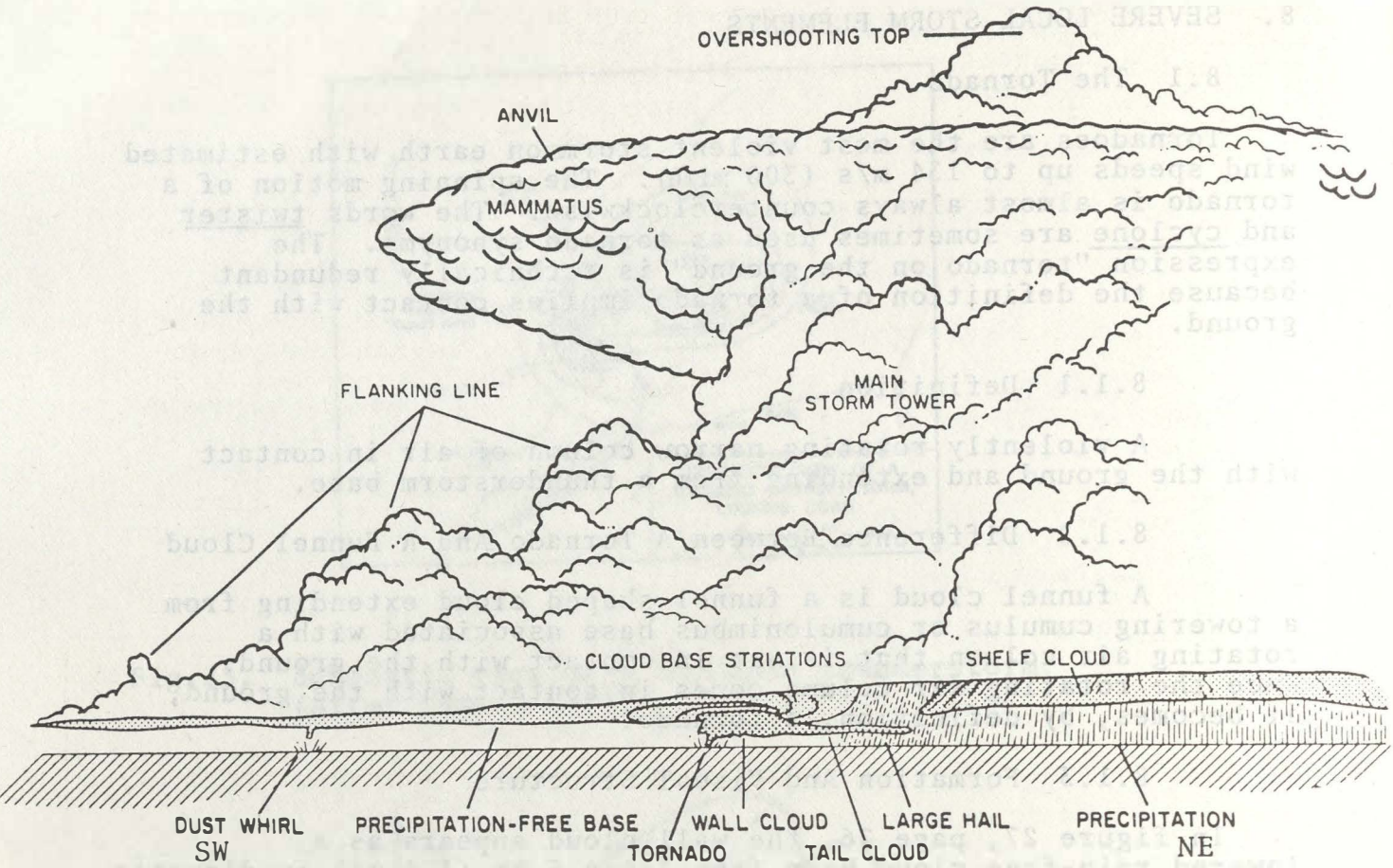

Fig.27. Composite view of a typical tornado producing cumulonimbus as seen from a southeasterly direction. Horizontal scale is compressed, and all the features shown could not be seen from a single location. (Diagram by C. Doswell)

8.1.4 Climatology

Tecson et al. (1979) computed that there was an average of 396 tornadoes per year from 1916 to 1978. Their statistics showed an increase in the annual number of tornadoes from 165 in the 1940's, 367 in the early 1950's to 605 by the late 50's and a record 1,110 tornadoes in 1973. McNulty et al. (1979) found the annual frequency of tornadoes to be increasing at a rate of 21 per year. Both studies suggest improved data reporting, public awareness, and increased population density as factors to be considered in the apparent increasing tornado frequencies of the 1970's.

Oklahoma City has experienced the most (200) tornadoes from 1916-1978 with Tampa, Dallas-Ft. Worth, Kansas City, and Houston all reporting more than 135 for the same period. Codell, Kansas, was struck three times in successive years, 1916, 1917, and 1918 on the same day, May 20th!

Tecson et al. (1979) found an average path length of 7.6 km (4.7 mi) for all tornadoes with the mean path length of the

weakest tornadoes being 2.3 km (1.4 mi) and the most violent tornadoes traveling 46 km (29 mi). The longest officially recorded tornado covered about 471 km (293 mi) through Illinois and Indiana on May 26, 1917, and lasted for 7 hours and 20 minutes!

The Wichita Falls tornado of 1979 had a width that varied from .8 km to 1.6 km (½-1 mi). A few tornadoes have exceeded 3.2 km (2 mi) in diameter.

Newton (1980) stated that in about 80% of tornado cases studied the path was less than 4.8 km (3 mi) long and 50 yards wide. Only 1 in 1000 tornadoes have wind speeds exceeding 116 m/s (260 mi/h) and over half have winds less than 45 m/s (101 mi/h).

One to two percent of all tornadoes produce most of the deaths and property damage. This one to two percent, in turn, represents only a small percentage of the 1% of all thunderstorms that produce severe weather, but are the tornadoes that we are most successful with in our forecasts and warnings.

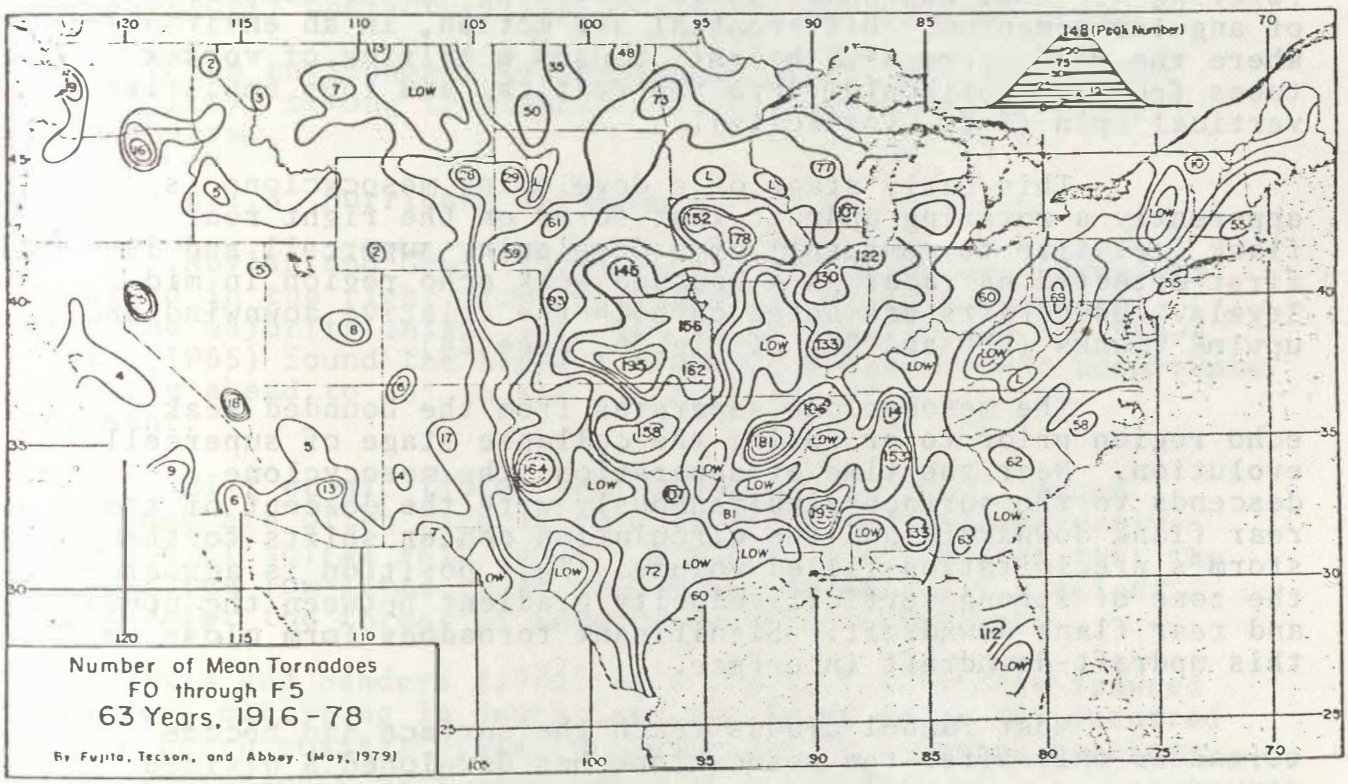

Fig.28. Tornado isolines. Note the association of maximum values with location of urban areas. (After Tecson et al.. 1979)

8.1.5 Mesocyclone Tornadoes

Doppler radar research during the 1970's has compiled convincing evidence that the small percentage of tornadoes producing most of the deaths and property damage are associated with small scale cyclones about 2-10 km (1-6 mi) in radius.

They are called mesocyclones or mesolows.

8.1.5.1 Mesocyclone Definition

A mesoscale cyclonic wind circulation, accompanied by a mesoscale low. The common type of mesocyclone is associated with the right rear of rotating thunderstorms, in the vicinity of the weak echo region. The rear of the mesocyclone is sometimes bounded by a radar hook echo.

8.1.5.2 Visual Indications

A mesocyclone sometimes is recognizable visually by rotation of the wall cloud (Fig.27, page 26) which is frequently the seat of intense vertical motion at low levels.

8.1.5.3 Evolution

The maximum tangential winds are roughly 20 m/s (45 mi/h) and are located in a circular band of counterclockwise rotating air that has spun inward according to the conservation of angular momentum. Differential air motion, in an environment where the wind veers with height, causes a tilting of vortex tubes from the horizontal into the vertical and thus amplifies vertical spin (i.e., vorticity).

This early stage of a developing mesocyclone is apparently a rotating updraft that forms on the right rear flank (relative to movement) of a developing supercell and is first detected on radar as a bounded weak echo region in mid-levels. Downdrafts are noted on both the relative downwind and upwind flanks (FFD and RFD of Fig.26, page 24).

The mesocyclone separates from the bounded weak echo region prior to or during the collapse stage of supercell evolution. Near the time of separation, the mesocyclone descends to the surface simultaneously with the descent of the rear flank downdraft and the circulation center shifts to the storm's precipitation-filled volume. This position is across the zone of strong vertical velocity gradient between the updraft and rear flank downdraft. Significant tornadoes form close to this updraft-downdraft interface.

Most funnel clouds reach the surface and become tornadoes only after the mesocyclone has developed a divided structure.

8.1.5.3.1 Tornado Cyclone

The tornado forms in a small tornado cyclone about 3-4 km (2-3 mi) in diameter which develops within the larger mesocyclone. The tornado cyclone is often detected by radar as an annular section of a cylinder, a dot, or small spiral.

8.1.5.3.1.1 Suction Vortex

Some tornadoes develop multiple vortices.

They are sub-tornado-scale vortices 5-50 m (about 6-55 yd) in diameter and are termed suction vortices (i.e., suction spots).

8.1.6 Gust Front Tornadoes

Brandes (1977) noted secondary mesocyclones or tornadoes forming along the trailing gust front (Fig.26, page 24) associated with the rear flank downdraft and analogous to waves along a synoptic scale cold front. (See "gust front" section on page 35.)

8.1.7 New Convection Tornadoes

Burgess and Donaldson (1979) documented the existence of small-scale tornadoes producing damage during the developmental stage of storms that later produced mesocyclones with additional tornadoes.

One tornado formed five minutes *before* the first radar echo. None of the storm's radar echoes indicated severe weather nor supercell characteristics in this developmental stage.

The environment was characterized by large thermal instability, strong tropospheric winds, and extreme vertical wind shears.

8.1.8 Hurricane Tornadoes

Novlan and Gray (1974) found most hurricane tornadoes occurred in the right front quadrant (relative to movement) with the majority inland some 185 km (100 nmi) from the shore. Smith (1965) found the highest probability of tornado occurrence directly ahead to 60° to the right of the direction of movement.

Hill et al. (1966) and Fujita et al. (1972) found tornadoes are often associated with the strongest convective elements of spiral rain bands. The author speculates that the tighter the low-level radar plan view reflectivity gradient, the greater the threat of tornadoes and/or downbursts.

Purvis and Sanders (1980) in a study of hurricane-spawned tornadoes occurring in South Carolina found about 70% occurred on the north coastal plain, probably due to enhanced boundary layer convergence over sand dunes in the area.

Phipps (1979) noted a classic hook echo on the wall cloud echo of hurricane Frederic as it moved inland on the Gulf Coast.

8.1.9 Cold Air Funnels

Cold air funnels are the result of an environment that includes relatively warm, moist air near the ground with a cold-core low pressure area aloft. Mesocyclones are not detected.

8.2 Hail

Hailstones range in size from 5 mm to 14 cm (0.2-5.5 in). They are frequently composed of alternate layers of clear and opaque (rime) ice.

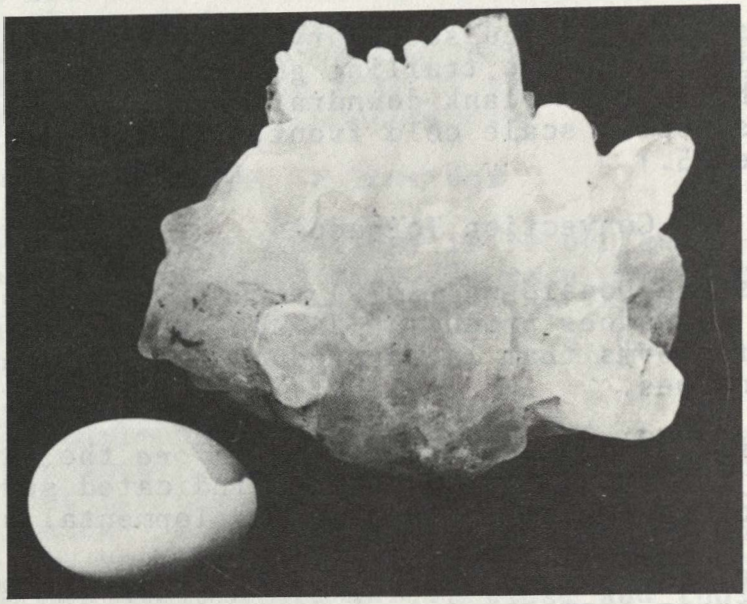

Fig.29. Coffeyville, Kansas, hailstone with maximum dimension of some 14 cm (5.5 in) and weight of 0.77 kg (1.7 lb). (After Knight and Knight, 1971)

8.2.1 Definition

Hail is precipitation in the form of balls or irregular lumps of ice, only produced by convective clouds.

8.2.2 Climatology

The principal hail area in the United States is along and to the lee of the eastern Rocky Mountains from New Mexico to Alberta, Canada. Fig. 30, page 31, is based on point frequencies and shows the average annual number of days with hail for the contiguous United States.

8.2.3 Evolution

The process by which hail receives its alternate layers of clear and rime ice is not completely known.

8.2.3.1 Rime Ice

The two conditions most favorable for the formation of rime ice are: (1) small drops and (2) instant freezing. Small bubbles become trapped, making the ice opaque. At times, bubbles will form after the ice is frozen; e.g., ice cubes often have bubbles that were not trapped but rather formed in place as the ice cooled. Rime ice is formed by the collision of small supercooled water droplets with hail embryos, usually graupel (i.e., snow pellets).

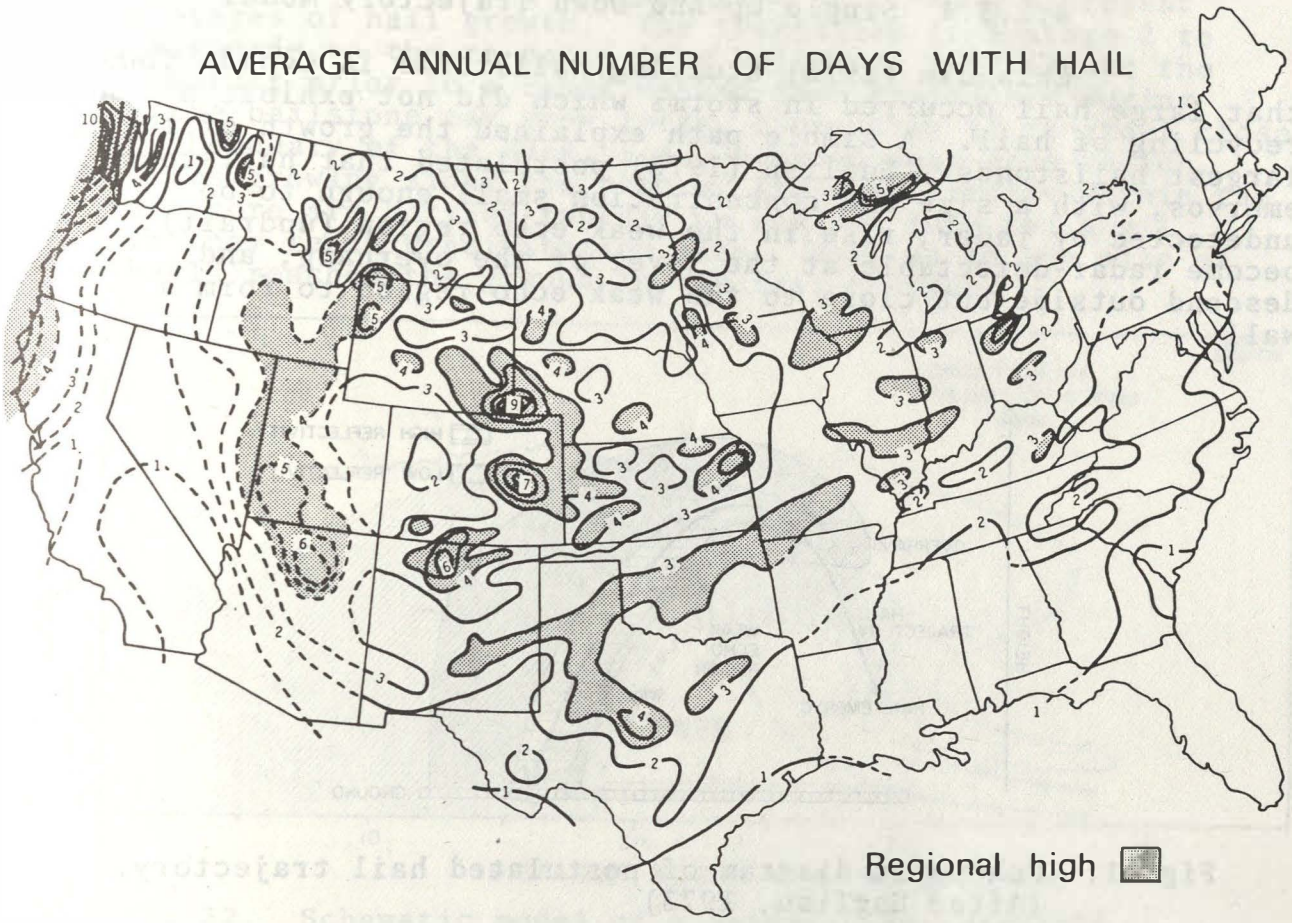

Fig.30. Average number of hail days per year. (After Changnon, 1977)

8.2.3.2 Clear Ice

The two conditions most favorable for the formation of clear ice are: (1) large drops and (2) slow freezing. Clear ice is formed by the collision of large, super-cooled water droplets with some object such as an airplane or a hailstone, or with other water droplets, as commonly occurs. Clear ice can also form by the refreezing of water on a hailstone surface when the stone is carried from below the freezing level (melting level) to above it.

8.2.3.3 Alternate Layers Of Clear And Rime Ice

Mason (1980) explains that when the diameter of ice crystals exceeds 0.1 mm (0.004 in), growth by collision with supercooled droplets will predominate. At low temperatures the impacting droplets tend to freeze quickly to produce pellets of soft hail containing large numbers of air bubbles, forming rime ice. When the growing pellet passes through a region of relatively high air temperature or high concentration of liquid water or both, the transfer of latent heat of fusion from the hailstone to the air cannot occur quickly enough to allow all the deposited water to freeze immediately. A layer of slushy ice forms, which may later freeze to form clear ice.

8.2.3.4 Single Up-And-Down Trajectory Model

Chisholm (1973) studying hailstorms in Canada found that large hail occurred in storms which did not exhibit a recycling of hail. A simple path explained the growth of the largest hailstones. English (1973) postulated that hailstone embryos, with a size and concentration small enough to be undetected by radar, rise in the weak echo region (updraft), become radar-detectable at the level of the overhang, and descend outside but close to the weak echo region to form a wall.

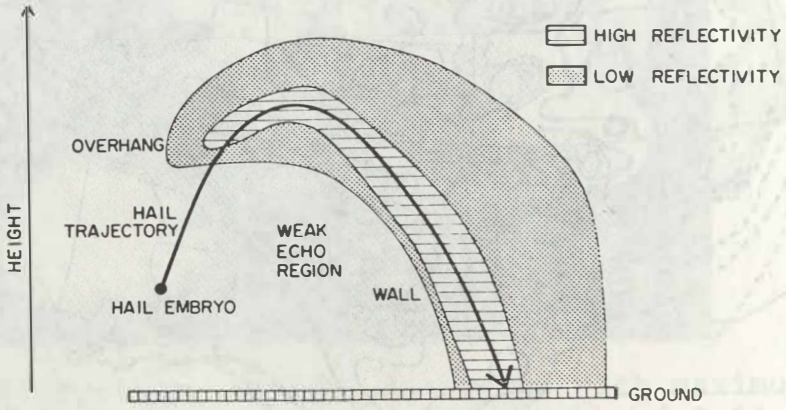

Fig.31. Schematic diagram of postulated hail trajectory. (After English, 1973)

8.2.3.5 Recycling And A Single Up-And-Down Trajectory Model

Browning (1977) listed three stages of hail growth in a unicellular supercell:

Stage 1 (First ascent)

Small particles are grown during a first ascent in a region of rather weak updrafts on the right flank of the main updraft.

Stage 2 (Recycling)

Some of these particles travel within weak updrafts around the forward edge of the main updraft before entering the core of the main updraft as embryos with a diameter of several millimeters.

Stage 3 (Single up-and-down trajectory)

Although there may be minor oscillations owing to small fluctuations in updraft intensity, these recycled embryos then grow into hailstones essentially during a single up-and-down trajectory.

In figure 32, trajectories 1,2, and 3 represent three stages of hail growth. The transition from stage 2 to 3 corresponds to the re-entry of a hailstone embryo into the main updraft prior to a final up-and-down trajectory during which the hailstone may grow large, especially if it grows close to the boundary of the BWER, i.e., bounded weak echo region. Particles growing along the path of the open circles within the updraft core are carried rapidly up and out into the anvil before they reach precipitation size. Hail up to the size of baseballs reached the ground in the hail cascade.

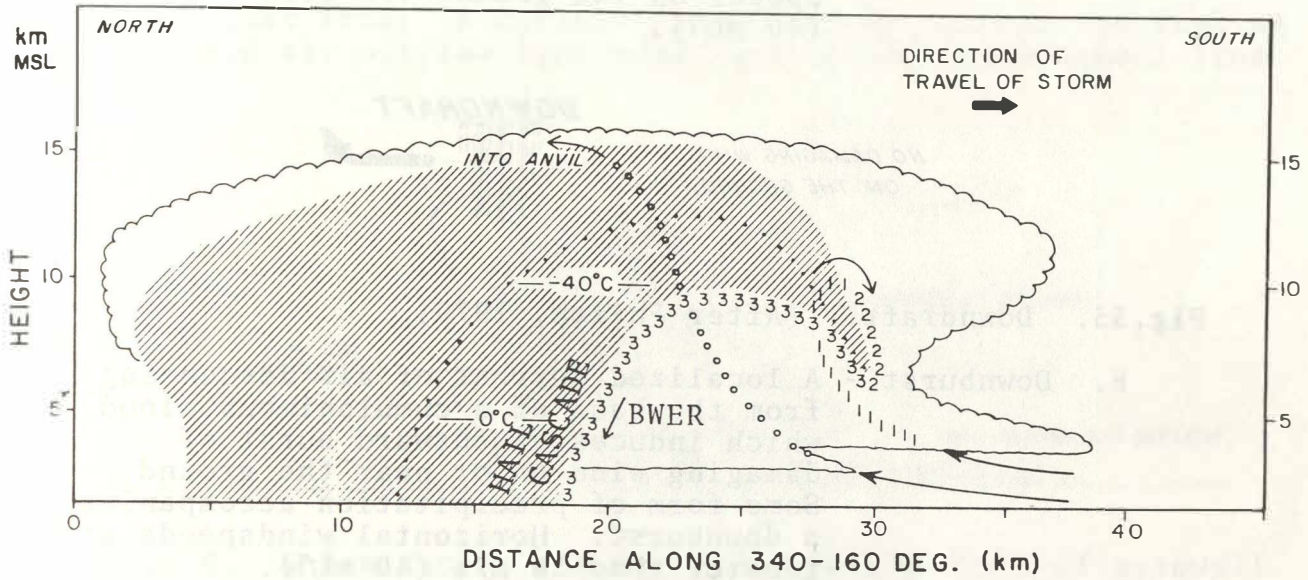

Fig.32. Schematic model of a unicellular supercell hailstorm. (After Browning and Foote, 1976)

8.2.3.6 Hail Production In A Supercell

Nelson (1980) examined hail production in supercell type storms and found a typical hail growth time of 10 minutes. Hail grew between 4-10 km (about 13-33 kft) with prime growth occurring between 6-8 km (about 20-26 kft). Favorable environmental temperatures ranged from -10 to -20°C. Temperatures warmer than -2°C were too warm and temperatures less than -25°C were too cold.

8.3 Wind

Damaging surface winds are often associated with severe thunderstorms. These winds are usually classified as tornado (highly convergent swirling winds affecting a relatively narrow path) or straight-line. Fujita and Wakimoto (1981) suggest a subclassification of straight-line winds into two categories, downburst and gust-front. Downburst winds are highly divergent, straight, or curved winds of damage-causing intensity. Straight-line winds are nondivergent winds of damage-causing intensity seen just behind an advancing gust front. Maximum downburst winds have been classified as F3, i.e., 70-92 m/s (158-206 mi/h). See appendix D for F-scale damage specifications.

8.3.1 Downdrafts, Downbursts, And Microbursts

Fujita (1978) proposed a classification of winds based on horizontal windspeeds and path length:

A. Downdraft - Relatively small-scale current of air with marked downward motion. A downdraft is encountered inside or below a cloud, but it does not induce a damaging wind on or near the ground. Horizontal windspeeds on the ground are less than 18 m/s (40 mi/h).

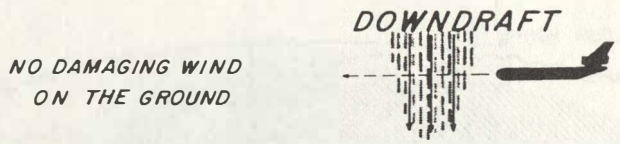

Fig.33. Downdraft. (After Fujita, 1979)

B. Downburst - A localized current of air descending from the base of a cumulonimbus cloud, which induces an outward burst of damaging wind on or near the ground. Some form of precipitation accompanies a downburst. Horizontal windspeeds are greater than 18 m/s (40 mi/h).

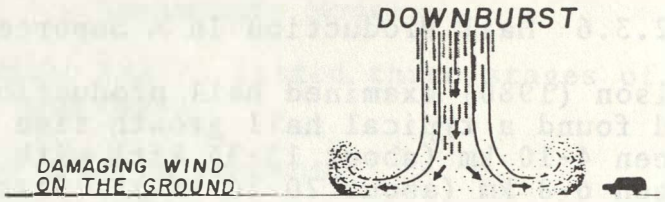

Fig.34. Downburst. (After Fujita, 1979)

C. Microburst - A mini-size downburst occurring with or without a downburst. Path length is less than 5.1 km (3.2 mi). By virtue of its small horizontal dimensions, a microburst induces a strong wind shear near the surface.

Fig.35. Microburst. (After Fujita, 1979)

8.3.2 Evolution

Clear air is entrained into a thunderstorm from outside, forced downward by gravitational pull, the drag of the falling precipitation, and evaporative cooling. The resulting downdraft/downburst air is denser than its surroundings. In general, the dryer the air mixed into a thunderstorm aloft, the greater the downdraft/downburst.

8.3.3 Gust Front

A gust front is defined as a boundary marking the leading edge of cold air outflow from individual storms in a squall line.

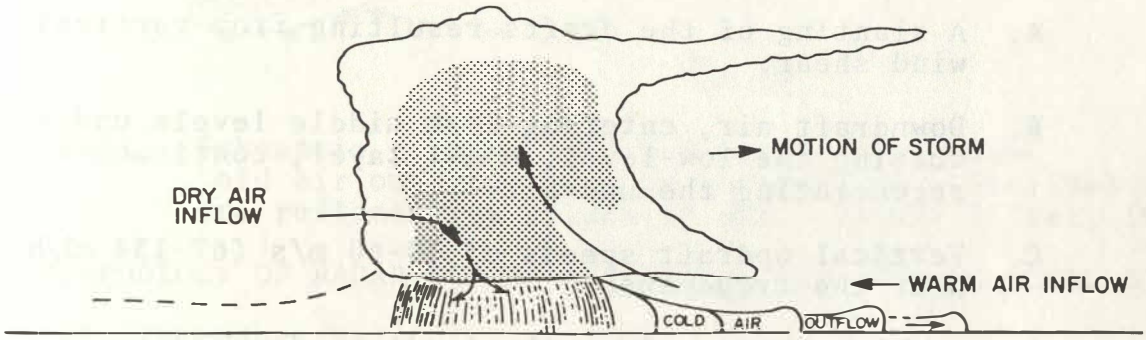

Fig.36. Schematic of the vertical cross-section of a squall line along the direction of motion. Stippling shows areas of rain and suspended precipitation aloft. Multiple surges in the gust front are shown. (After Goff, 1976)

8.3.3.1 Characteristics

Goff (1976) in a study of 20 Oklahoma gust fronts found most were dry with precipitation following, on the average, about 4 to 18 minutes after passage. Wind gusts in the cold air were about 1½ times the speed of movement. Gust fronts tend to form parallel to squall lines due to cold air outflow and are marked by strong shears in the horizontal and vertical winds. A pressure rise usually was observed first followed by a windshift and then a temperature break. Fankhauser et al. (1982) characterizes gust fronts in northeast Colorado in terms of a temperature discontinuity followed by a wind shift about 3 minutes later with the peak gust occurring 12 minutes, on the average, after the temperature break.

9. THE SQUALL LINE

9.1 Introduction

Severe weather producing squall lines are most common in spring and early summer. They rank next to hurricanes in casualties and damage caused but also supply most of the beneficial rainfall in some regions.

9.2 Squall Line Definition

Any line or narrow band of active thunderstorms.

Squall lines may extend over several hundred kilometers and consist of many laterally aligned cells which do not disruptively interfere with one another. Cells can be ordinary, nonsevere or severe multicell, supercell, or a combination of these.

9.3 Evolution

Squall lines tend to form in unstable air rich in water vapor in the lowest 1-3 km (about 3-10 kft). Newton (1980) listed circulation characteristics as:

A. A slanting of the drafts resulting from vertical wind shear.

B. Downdraft air, entering from middle levels undercutting the low-level, moist layer, continuously regenerating the updraft.

C. Vertical updraft speeds of 30-60 m/s (67-134 mi/h) near the tropopause.

Propagation occurs along the leading edge and may be either discrete, i.e., beginning and ending during the life of the squall line, or continuous. Individual storms tend to move with the mean environmental winds, but overall line movement is usually to the right of storm motion due to growth starting on the southernmost end of the line while the northern end dissipates.

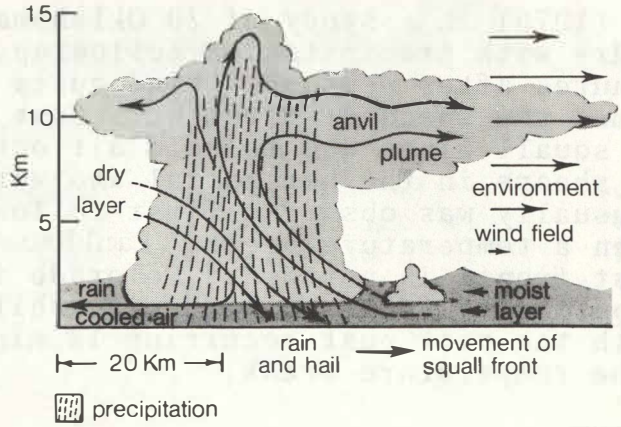

Fig.36. Section through squall-line-type thunderstorm. (After Newton, 1980)

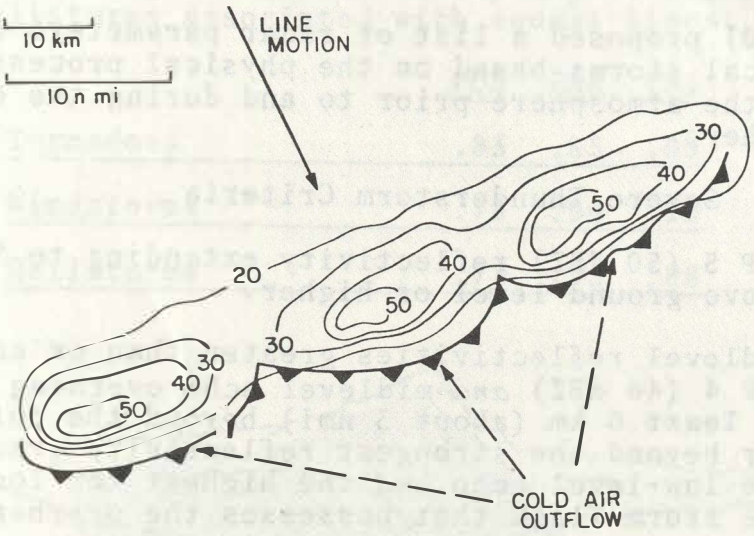

Fig.37. Schematic of squall line in radar plan view. Cold air outflow shown as barbed line. Isolines are reflectivity values in dBZ. (After Zittel, 1978)

10. MORPHOLOGY OF RADAR ECHOES ASSOCIATED WITH SEVERE LOCAL STORMS

10.1 Introduction

This section on radar echoes associated with severe local storms is based on observations made with conventional radar by people looking at horizontal (PPI) views displayed in polar coordinates and vertical (RHI) views displayed in rectangular coordinates. Remoted radar data consist only of the horizontal view converted to rectangular coordinates. *Caution*, the resulting loss of information reduces the usefulness of remoted radar data for detecting echoes associated with severe local storms.

It is important to be aware of the radar antenna elevation angle. A change of just 1° up or down usually results in the displayed horizontal view being several kilometers above or below the initial elevation angle. Also, under standard atmospheric conditions the radar beam is constantly gaining altitude with increasing range from the radar site. This results in the more distant echoes representing conditions several kilometers above ground level. (See appendix E for midpoint height of radar beam under standard conditions.)

If the radar data are from a 5-cm radar, be aware that significant storms can virtually disappear because of signal attenuation from nearby front-line storms.

In general, radar data are most useful and representative of actual weather conditions to a range of 138 km (75 nmi).

10.2 Severe Thunderstorm And Tornado Criteria

Lemon (1980) proposed a list of radar parameters associated with severe local storms based on the physical processes which take place in the atmosphere prior to and during the occurrence of severe weather.

10.2.1 Severe Thunderstorm Criteria

A. VIP 5 (50 dBZ) reflectivity extending to 8 km (26 kft) above ground level or higher.

B. Midlevel reflectivities greater than or equal to VIP 4 (46 dBZ) *and* midlevel echo overhang extending at least 6 km (about 3 nmi) beyond the outer edge of (or beyond the strongest reflectivity gradient of) the low-level echo *and* the highest top located over the storm flank that possesses the overhang.

10.2.2 Tornado Criteria

A. Existence of an authentic hook echo. (See "hook and hooklike echoes" section beginning on page 48.)

B. Detection of a bounded weak echo region when all the criteria listed under B. of severe thunderstorm criteria have been met. (See appendix F for radar tilt scan sequence.)

The parameters were tested on 80 cases in Oklahoma with a resulting probability of detection (POD) = .93, false alarm ratio (FAR) = .24, and critical success index (CSI) = .71. (See appendix G for probability of detection, false alarm ratio, and critical success index.)

10.3 Squall Lines

10.3.1 Radar Characteristics

Lemon (1980) found the part of the line that is most likely to be severe indicated by:

A. A strong low-level reflectivity gradient.

B. A midlevel echo overhang.

C. A shift in the echo top from over the low-level reflectivity core to along the leading edge of the line.

Radar lines are typically 20-50 km (11-27 nmi) wide and a few hundred to 2000 km (1080 nmi) long. Average movement is 15 m/s (34 mi/h) for 6-12 hours or more. Echo tops are frequently 10-15 km (33-49 kft).

10.3.2 Severe Weather

Bigler (1955) reported a probability of detection of

.82 for tornadoes associated with squall lines. Donaldson (1975) listed the following results in attempting to forecast tornadoes, wind, and hailstorms associated with squall lines:

	POD	FAR	CSI
Tornadoes	.83	.95	.05
Windstorms	.78	.90	.10
Hailstorms	.73	.92	.08

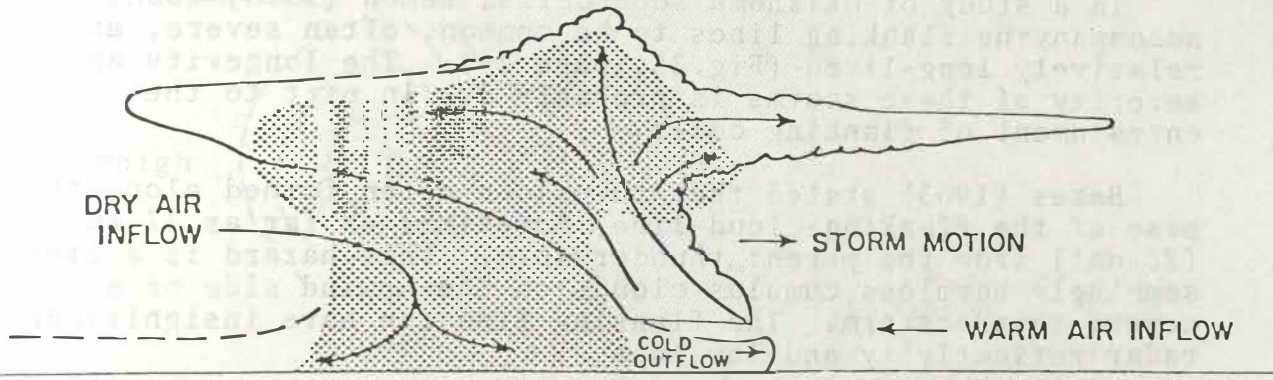

Fig.38. Vertical cross section through a severe squall line. The cross section is oriented normal to storm motion. Included are the precipitation echo (stippled) as well as the cloud, drafts, and location of the surface gust front created by the outflow. (After Wilk et al., 1978)

10.4 New Echoes Forming In An Established Squall Line

Whiton and Hamilton (1976) state that in an established squall line, the genesis region most likely for severe local storms to form is the southern end of a line for lines oriented north to south.

10.5 Pivoting Squall Line

10.5.1 Definition

A squall line pivoting around a fixed point.

The end of the line farther from the pivot point moves faster than the end of the line nearer the pivot point.

10.5.2 Radar Characteristics

A. VIP 5 or VIP 6 echoes.

B. Echo tops quite high.

10.5.3 Severe Weather

Whiton and Hamilton (1976) state that normally, the faster moving end is in the northern part of the line and will produce greater than normal surface gustiness. Tornadoes and hail are also possible.

10.6 Gust Fronts

Dry gust fronts can sometimes be detected as a thin or fine line, especially with the sensitivity time control (STC) turned off. (See "gust front" section on page 35.)

10.7 Flanking Line

In a study of Oklahoma supercells, Lemon (1976) found the accompanying flanking lines to be common, often severe, and relatively long-lived (Fig.25, page 24). The longevity and severity of these storms is probably due in part to the entrainment of flanking cells.

Bates (1963) stated that tornadoes often formed along the base of the flanking-cloud-line, sometimes as far as 37 km (20 nmi) from the parent thunderstorm. This hazard is a line of semmingly harmless cumulus clouds on the upwind side of a severe thunderstorm. The flanking line can have insignificant radar reflectivity and low tops.

10.8 Dry Line Severe Thunderstorms

Burgess and Davies-Jones (1977) studied severe thunderstorms associated with dry lines in eastern Oklahoma. They found intense updrafts at the rear of the storms along a flanking-type line with tops to 4 km (13 kft) above the lifted parcel equilibrium level (i.e., layer of increasing stability).

10.8.1 Radar Characteristics

A. Small, weak low-level echoes less than or equal to VIP 4.

B. No hook echoes.

C. No evidence of supercell development.

10.9 Line Echo Wave Pattern

Perhaps the most significant line radar pattern that indicates severe weather is the line echo wave pattern (LEWP).

10.9.1 Definition

Nolen (1959) defined a LEWP as a configuration of radar echoes in which a line of echoes has been subjected to an acceleration along one portion and/or a deceleration along that portion of the line immediately adjacent, with a resulting sinusoidal mesoscale wave pattern in the line.

Forbes (1978) classifies the LEWP as a "distinctive echo". (See "echoes associated with mesocyclones" section beginning on page 50.)

10.9.2 Evolution

Hamilton (1969) proposed that the part of the LEWP trailing farthest behind and forming the sharp bend (crest) is formed by a mesolow and that the acceleration of the line is accomplished through a spreading out of the mesohigh. This is often called the bulge or bow echo. (See "bow echoes" section beginning on page 43.)

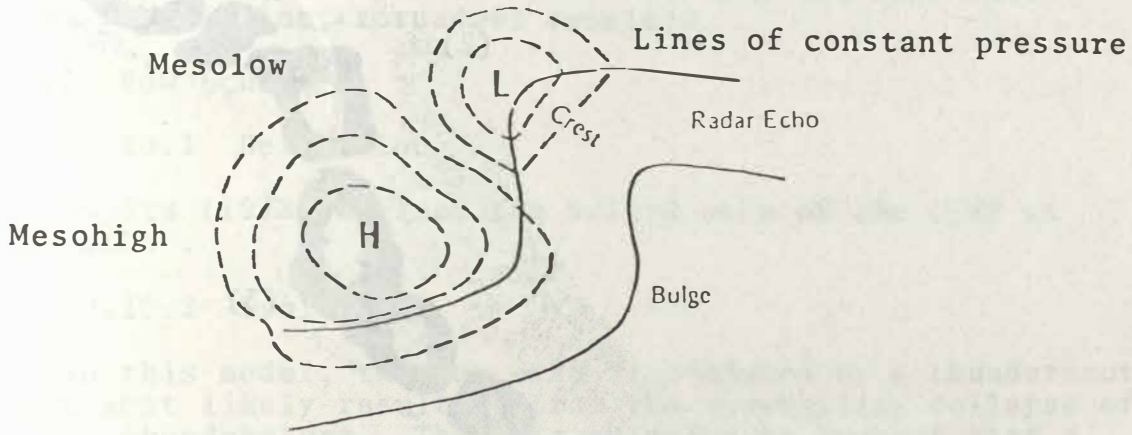

Fig.39. Proposed pressure pattern and LEWP formation. (After Hamilton, 1969)

10.9.3 Radar Techniques

A LEWP is often not easy to detect on the plan position indicator (PPI) scope in the linear (LIN) or logarithmic (LOG) mode because of intervening lighter precipitation. You may find it necessary to attenuate the returned signal by several decibels (dB). Some radar operators start with 3 dB of attenuation and increment in 3 dB steps until the LEWP is outlined. Selection of the contoured log (C-LOG) mode usually outlines a LEWP characterized by VIP 4 or higher reflectivities.

It is sometimes important to tilt the antenna a few degrees to midlevels to detect a developing LEWP. The increased resolution of short pulse or the off-center PPI feature can also be useful.

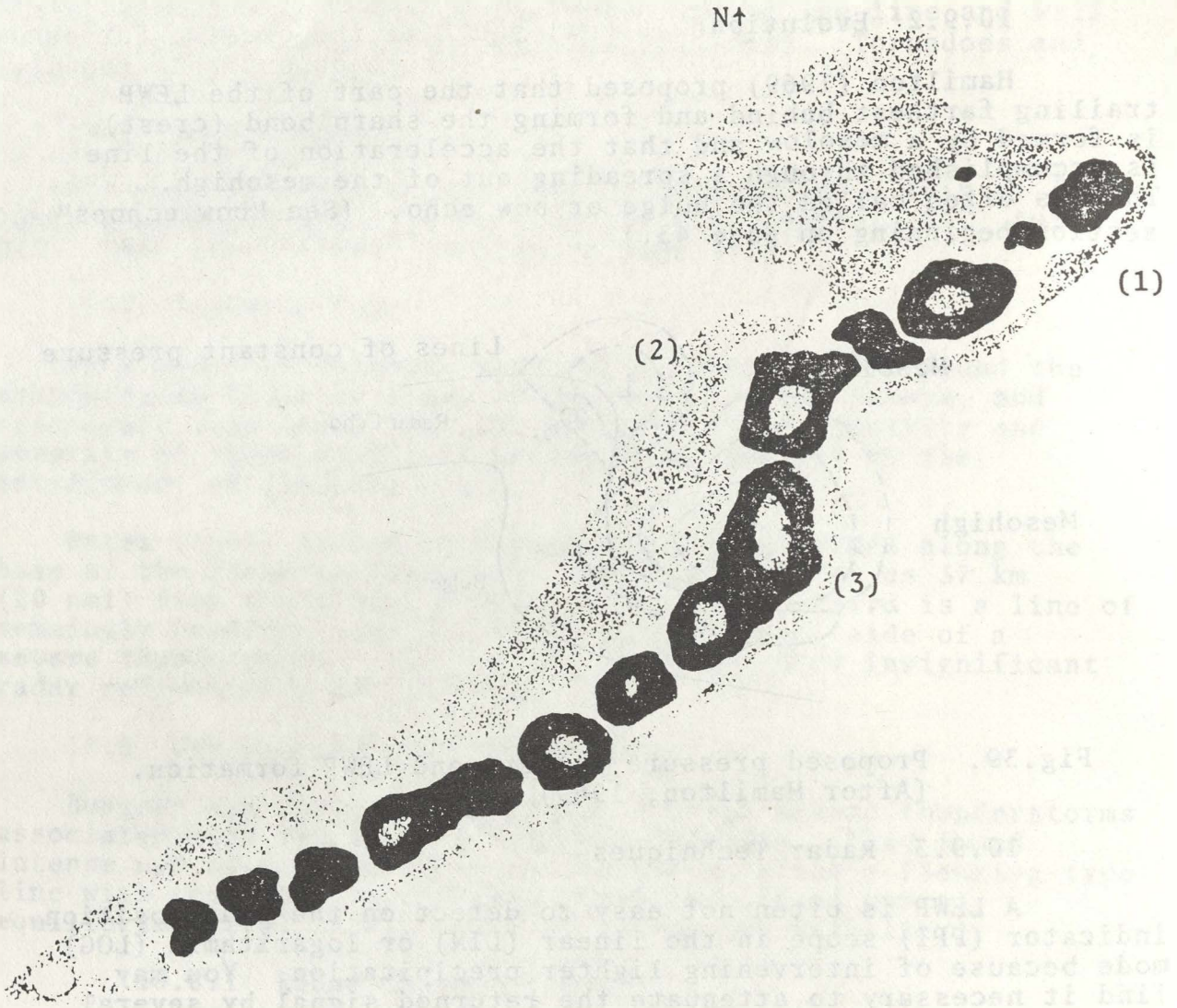

Fig.40. Schematic of LEWP as depicted on PPI scope in C-LOG.

10.9.4 Severe Weather

Galway (1967) suggested the following interpretation of the LEWP (shown in figure 40):

A. Tornadoes are most likely at the crest (2) and slightly south of that point.

B. Severe thunderstorms, particularly hail and strong surface winds at (3).

C. Hail and strong surface winds also at (1), but less likely than at (3). However, if point (1) is moving faster than point (3), severe weather becomes at least as likely there as it is at (3).

Nolen (1959) found that tornadoes occurred near the wave crest in three-fourths of cases studied. Cook (1961) found that 40 of 49 LEWP's had severe weather with the most favorable

distance being 19-74 km (10-40 nmi) south of the crest. Forbes (1978) in a study of the April 3rd, 1974, tornado outbreak found tornadoes associated with LEWP's form near the center of the main echo or west to southwest of it.

Cook (1961) investigating density of coverage of LEWP's found tornadoes most frequently associated with scattered or broken lines. Most windstorms occurred with solid lines and most hailstorms occurred with scattered lines. In 8 out of 19 cases where cells developed in front of lines and were later overtaken by the line, tornadoes resulted.

10.10 Bow Echoes

10.10.1 Definition

Fujita (1978) defined the bulged echo of the LEWP as the "bow echo".

10.10.2 Evolution

In this model, the bow echo is produced by a thunderstorm downburst most likely resulting from the snowballing collapse of a majestic thunderstorm. There is evidence to suggest that a large, strong, tall (LST) thunderstorm reverses its airflow direction upsidedown, upon reaching a critical point of no return. The final stage of the evolution of a bow echo is the comma echo stage. Usually a comma echo appears during the weakening stages of downbursts.

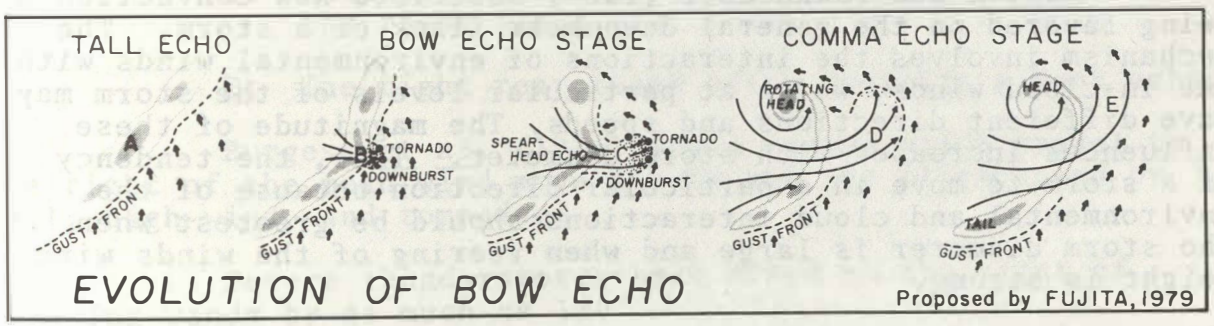

Fig.41. Model of the evolution of a bow echo. The final stage of this evolution is a comma echo which can be identified on a PPI scope quite often. (After Fujita (1979)

10.10.3 Radar Characteristics

A. Bow echoes are often embedded within LEWP's.

B. Echoes on the bow move faster than those near both edges.

C. The most intense downbursts are likely to occur near the forward center of the bow.

D. The bow has a spearhead or kink pointing towards the direction of motion denoting the strongest downburst.

E. Bow echoes have a tendency to move fast while deviating to the right.

10.10.4 Environment Characteristic

The direction of the bow echo often coincides with the wind direction at the tropopause.

10.11 Echo Movement

10.11.1 Translation Or Propagation?

Echo movement is due to translation or propagation or both.

Translation is echo movement with the steering wind. It is useful to think of the thunderstorm echo as a balloon being steered by the environmental winds.

Propagation refers to the apparent movement of a storm through generation and dissipation. Forbes (1978) defines discrete propagation in terms of new cells forming at irregular intervals.

10.11.2 Factors Influencing Echo Movement

Newton and Fankhauser (1964) described new convection as being favored on the general downshear flank of a storm. The mechanism involves the interactions of environmental winds with the in-cloud winds, which at particular levels of the storm may have different directions and speeds. The magnitude of these influences increases with storm diameter. Thus, the tendency of a storm to move in a particular direction because of the environmental and cloud interactions should be greatest when the storm diameter is large and when veering of the winds with height is strong.

Newton (1963) found the motion of single cells or small clusters closely related to the wind velocity at 3 km (about 10 kft) or the mean wind between 1½-6 km (5-20 kft).

Weaver (1979) lists three factors influencing echo movement:

A. The mean cloud-layer wind vector.

B. The strength, orientation, and movement of boundary-layer convergence zones.

C. Thunderstorm-induced convergence zones.

Caution is advised in calculating storm motion from the movement of echo centroids. The echo may expand downwind in time as an area of rain or small hail, but the region significant to severe local storms may not be moving at all, or moving quite differently from the centroid.

10.11.3 Anomalously Moving Echoes

10.11.3.1 S–R Supercell

Browning (1964) defined the term "severe right-moving" supercell from the radar indication that most severe local storms propagate anomalously to the right of steering winds and of weaker storms in the area. They tend to travel slower than the mean tropospheric winds.

Fujita and Bradbury (1966) found that all tornado producing echoes in the Palm Sunday outbreak moved to the right of the direction of the 500-mb winds while echoes that did not produce tornadoes moved generally in the direction of the stream lines of the 500-mb winds.

Burgess (1974) using Doppler radar to examine the structure of severe local storms in Oklahoma listed the following characteristics of a S–R supercell:

A. There is one dominant cell that moves to the right of the mean winds.

B. Continuous propagation occurs on the right flank.

C. Extensive midlevel echo overhang exists along the right flank.

D. The right rear flank often contains a hook echo.

Burgess et al. (1976) found storms which travel to the right of the mean wind move slowly and are accompanied by hail, high wind, and tornadoes.

Severe thunderstorms have moved to the right of steering winds by as much as 180°.

10.11.3.2 S–L Supercell

Hammond (1967) investigated the "severe left-moving" supercell. The S–L supercell moves faster than the S–R supercell and most often results from a splitting thunderstorm.

Burgess et al. (1976) found S–L supercells move with an average speed of 19 m/s (43 mi/h) as opposed to 12 m/s (27 mi/h) for S–R supercells.

S–L supercells tend to be accompanied by hail and high winds, but are less likely to produce tornadoes than the S–R supercells.

10.11.4 Deviation Theories

Goldman (1966) describes the kinematics of motion useful in explaining the deviate motion of severe local storms from a path parallel to the steering winds.

The Bernoulli principle indicates that on the side of the storm where the relative wind speed is the greatest, the pressure will be the lowest, with a resultant force perpendicular to the wind field and toward lower pressure. This means, the slower the movement of the storm, the greater the deflection to the right or left depending on whether cyclonic or anti-cyclonic rotation is occurring.

Many researchers studying the circulation and structure of severe local storms agree that a substantial number rotate cyclonically. A cyclonically rotating cloud embedded in a wind field should experience a deflective force at a right angle to the relative wind direction. The deflection, for a cyclonically rotating cylinder in a uniform flow field, is described by the Kutta-Joukowski theorem or the Magnus effect.

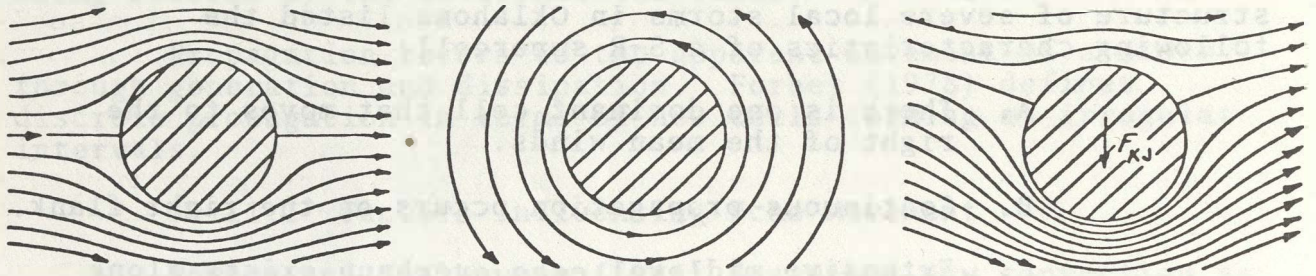

(a) Streaming flow past a barrier

(b) Circulation about the barrier

(c) Sum of (a) & (b). Note the direction of the force.

Fig.42. The general kinematics of motion related to the Kutta-Joukowski force. (After Goldman, 1966)

10.11.4.1 Forces On AnS-R Supercell

A. Cyclonic rotation has the effect of producing a storm motion to the right having a speed lower than the mean wind.

B. The low-level relative inflow, as increased by cyclonic rotation, in the rear-right quadrant of the storm under strong veering wind conditions should produce continuous propagation, which has the effect of decreasing the translational speed and producing the storm component of motion to the right.

C. An additional force arises from the Kutta-Joukowski force. This force could account for a substantial part of the right deviation.

10.11.4.2 Forces On An S-L Supercell

Burgess et al. (1976) speculated that a vector combination of rotation influence and propagation are responsible for the observed deviate motion of the S-L supercell. Anticyclonic rotation of the updraft was discovered at storm midlevels.

10.11.5 Echo Speed As An Indicator For Storm Severity

10.11.5.1 Yea

Stout and Hiser (1955) found that high echo speeds are associated with damaging winds.

10.11.5.2 Nay

Brandes (1972) studied 104 storms and found the average speed of 54 severe local storms to be 27 knots (31 mi/h), while 50 nonsevere storms also had an average speed of 27 knots.

10.11.6 Converging Echoes

Stout and Hiser (1955) found a high degree of association of echo convergence and vortex motion with tornadoes, severe winds, and hail. They also found that cell merger in a tropical air mass usually only produces heavy precipitation.

Staats and Turrentine (1956) found strong convergence of echoes associated with tornado producing storms in Oklahoma and Kansas.

Forbes (1978) speculates that the downdraft of the merging cell acts as a source of vorticity to enhance a mesocyclone.

Lemon (1977) concludes that most severe weather associated with a storm is a result of the storm's character and *not* due to merger with other storms.

10.11.7 Splitting Echoes

Burgess et al. (1976) list four stages of a storm split:

A. The formation stage - A thunderstorm develops and propagates generally eastward or northeastward, not necessarily in the direction of the mean wind. A pronounced reflectivity gradient appears along the storm's rear flank.

B. The elongation stage - The thunderstorm elongates to an elliptical shape with the major axis of the ellipse generally perpendicular to the direction of storm movement. Splitting of the intense reflectivity core is observed. The "split cores" grow apart and reflectivity gradients intensify along the left and right storm flanks.

C. The splitting stage - The central part of the echo rapidly diminishes in size and intensity. This dissipation leaves two separate thunderstorm cells.

D. The deviate stage - Relative to the direction of motion, the left member veers sharply to the left of the mean wind and increases in speed. The right member veers to the right of the mean wind and decreases in speed.

Examination of 32 splitting storms in the same study revealed:

A. The approximate lifetime exceeded 2½ hours.

B. The average deviation from the mean wind was 28° for the left moving storms and 24° for the right moving storms.

C. In 26 of the storms, 3 of the left movers produced tornadoes while 9 of the right movers produced tornadoes. *All* 26 splitting storms produced hail 3/4 inch or greater.

10.12 Hook And Hooklike Echoes

10.12.1 Introduction

In 1945 an association was made between an unusually shaped radar echo and a tornado at Maxwell Air Force Base, Alabama. The radar shape was described as being that of a figure "6".

Brooks (1949) related the figure "6" to a small scale cyclone with the following characteristics:

A. The tornado resulted from a cyclone 19-37 km (12-23 mi) in diameter.

B. The tornado cyclone forms on the rear right side (relative to movement) of a rotating thunderstorm.

C. The circulation draws precipitation from the main echo into the flow around the small scale cyclone.

Brook's small scale cyclone is known today as a mesocyclone. Doppler radar has shown the average diameter of a tornado-producing mesocyclone to be 4-20 km (about 2-12 mi).

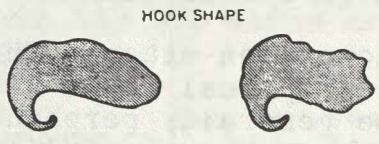

Fig.43. Linear PPI display of hook shape. (After Fujita, 1973)

10.12.2 Hook Echo Characteristics

Sadowski (1969) studied 46 hook echoes and found:

A. The tornado was located in the knob of the hook echo in 29 of 33 cases.

B. There were 13 cases of hook echo detection *before* the tornado was reported with a time range of 5 to 30 minutes, 8 cases of simultaneous occurrence, and 5 cases where the tornado was reported before the hook echo was detected with a time range of 8 to 27 minutes.

C. The hook forms in a short time, usually only a few minutes.

D. The average hook moves with a speed of 27 knots (31 mi/h).

E. In 37 cases, the shortest hook echo duration was 5 minutes while the longest was *3 hours and 20 minutes*. The average hook echo persisted for 30 minutes.

F. In this study, 40 out of 46 hook echoes were associated with tornadoes.

10.12.3 Hook Echo Shapes

Fujita (1973) defined a family of hook echo shapes:

A. Pendant - Large, solid echo with a small pendant finger attached. May be difficult to distinguish from random configuration.

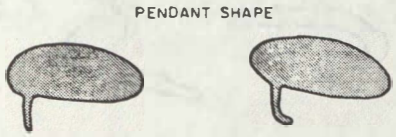

Fig.44. Linear PPI display of pendant shape. (After Fujita, 1973)

B. Classic hook - Fish hook shape. Parent cell will become deformed due to stronger circulation.
(See figure 43, page 48.)

C. Doughnut - Develops when the hook wraps around in such a manner that the tip connects to the parent echo, forming an eye at the center of circulation.

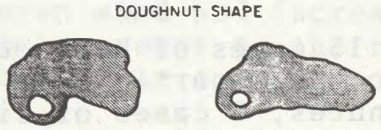

Fig.45. Linear PPI display of doughnut shape. (After Fujita, 1973)

D. Bird shape - The parent cell continues to deform and the entire cell structure becomes influenced by the tornado cyclone center. The "V" notch appears. Sometimes called the flying eagle or V-shape.

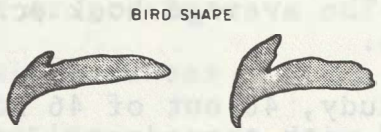

Fig.46. Linear PPI display of bird shape. (After Fujita, 1973)

E. Spiral - May occur when another cell is nearby to the south. The precipitation from the second cell is drawn into the circulation.

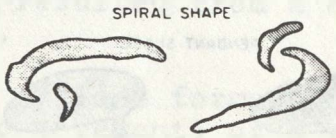

Fig.47. Linear PPI display of spiral shape. (After Fujita, 1973)

10.12.4 Echoes Associated With Mesocyclones

Forbes (1978) in a study of the April 3, 1974, tornado outbreak defined a set of echoes associated with mesocyclones as "distinctive echoes":

A. Appendage - An echo protrusion on the right rear, oriented at least 40° to the right of echo movement.

B. Hooklike - An echo whose appendage is in the form of a thin line, arc, or incomplete hook oriented 60°-80° to the right of echo movement.

C. Hook - An echo whose appendage is at an orientation in excess of 80° to the right of echo movement or in a classic hook shape.

The classic hook outlines the mesocyclone associated with the main updraft. Tornadoes generally form as the shape of the appendage becomes more like a hook or when echoes merge onto the rear of the hook.

D. Line echo wave pattern - Included to make the list of echoes associated with mesocyclones complete. Information on LEWP's begins on page 40.

10.12.4.1 Tornadoes Associated With Distinctive Echoes

Forbes (1978) also found that tornadoes associated with distinctive echoes tend to be stronger and last longer than those from nondistinctive echoes. Out of 55 distinctive echoes, 36 (65%) were tornadic. 81% of these tornadoes occurred with well-formed hook echoes, echoes with hooklike appendages or the main echo in a line echo wave pattern.

10.12.4.2 Classification Of Low-level Echoes In April 3, 1974, Tornado Outbreak

Forbes (1978) classified 55 echoes in terms of cells. 33 were supercells, 14 multicells, 3 associated with line echo wave patterns, and 5 were uncertain as to classification

10.12.4.3 Radar Characteristics For Tornadic And Nontornadic Storms Of April 3rd.

TORNADIC	NONTORNADIC
1. Began as small echo and grew rapidly.	1. Began as small echo.
2. Was apparently a supercell.	2. Was a supercell or multicell.
3. Formed an appendage 70 minutes after echo formed.	3. Formed an appendage 49 minutes after echo formed.
4. Possessed an appendage 145 minutes.	4. Possessed an appendage 62 minutes.
5. Was hooklike for 50 min.	5. Was hooklike for 2 minutes.
6. Classic hook 16½ min.	6. Seldom showed classic hook.
7. Made a left turn as echo weakened and decayed.	

10.12.5 Measurement Of Hook Echoes

Sadowski (1969) using a measurement technique called the "circle of best fit" found the largest diameter of 46 hook echoes to be 22 km (12 nmi) with an average of 13 km (7 nmi). The distance from the edge of the parent echo to the extremity of the hook was rarely more than 18.5 km (10 nmi) and never more than 28 km (15 nmi). (See appendix H for Sadowski's tornado warning technique.)

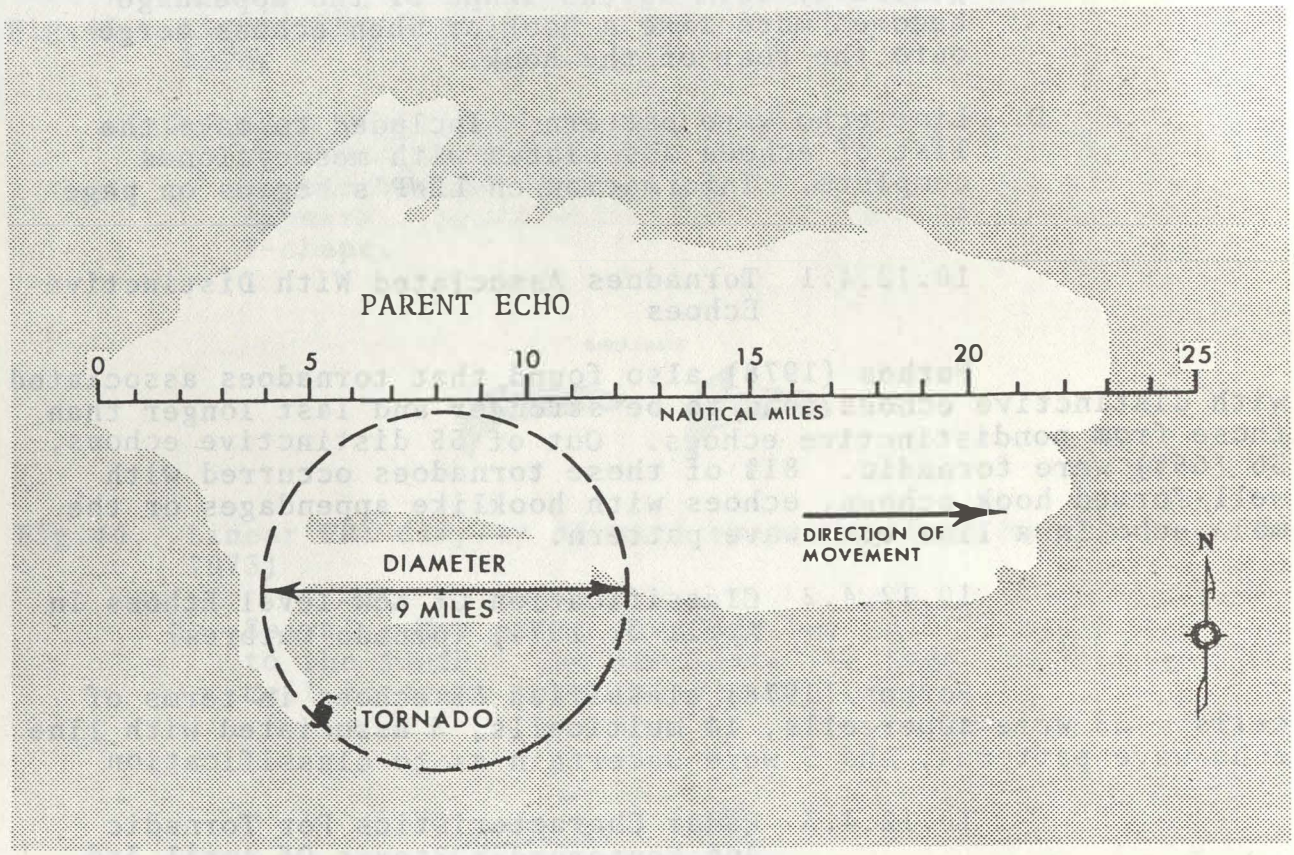

Fig.48. Measurement of hook echo by circle of best fit. Linear PPI display. (After Sadowski, 1969)

10.12.6 Radar Techniques For Hook Echo Detection

Fujita's family of hook echo shapes is defined relative to a PPI display in the LIN or LOG mode. Many operators have found it useful to elevate the antenna up to 3° and attenuate the signal to block out lighter, intervening precipitation. Doppler radar studies during the 1970's have shown funnels forming in midlevels and then descending to the ground. Cross-section studies of range height indicator profiles have shown some hooks to extend as high as 11-12 km (about 36-39 kft) above ground level. Use of the short pulse and off-center PPI features will often increase the chances of hook echo detection.

10.12.7 Normal Radar Range Of Hook Echo Detectability

Forbes (1978) found the normal range of hook echo detectability to be 111 km (60 nmi). One hook echo was detected at an extreme range of 228 km (123 nmi) during the April 3, 1974 tornado outbreak.

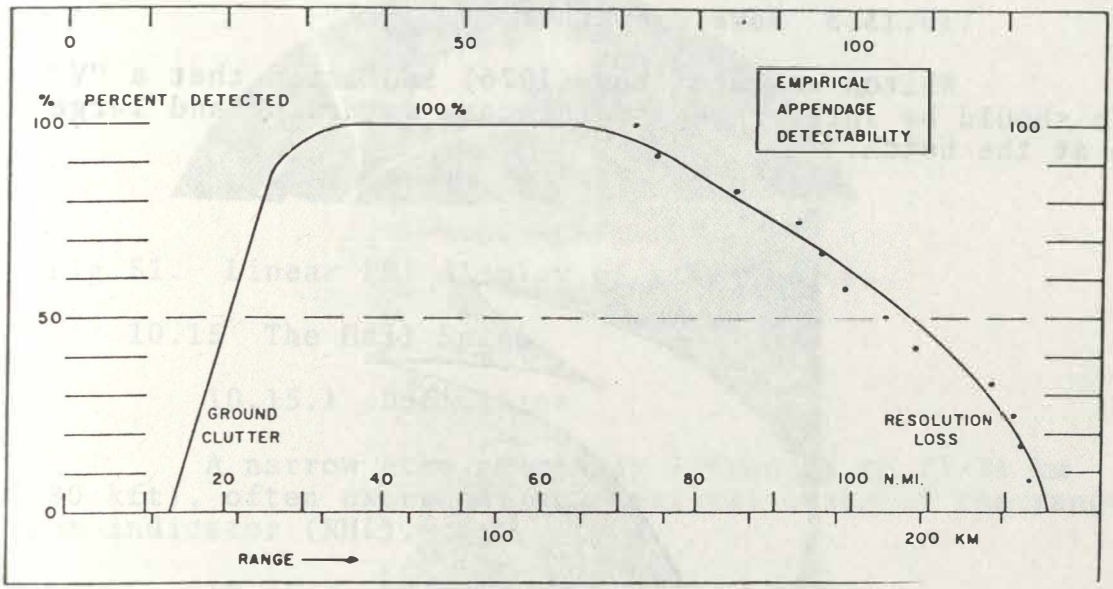

Fig.49. Empirical appendage detectability. (After Forbes, 1978)

10.12.8 Hook Echoes Associated With Waterspouts

Forbes (1978) reported that 10% of confirmed waterspouts are associated with hook echoes.

10.12.9 Critical Success Index

Donaldson et al. (1975) determined the following results in forecasting tornadoes from the presence of hook echoes:

POD	FAR	CSI
.50	.10 to .25	.43 to .47

10.13 "V" Notch

10.13.1 Evolution

The "V" notch may be formed by:

A. The merging of two echoes into a single large echo, forming a "V" at the point of merger.

B. Midlevel divergence of environmental flow around a supercell.

10.13.2 Radar Characteristics

The "V" notch may form on the downwind side of a single echo while the trailing half of the echo may have a protrusion or pendant that can develop into a hook echo. The "V" notch in this case is best interpreted as supporting evidence of a hook echo.

10.13.3 Severe Weather

Whiton and Hamilton (1976) indicated that a "V" notch should be interpreted to indicate a tornado and large hail at the notch.

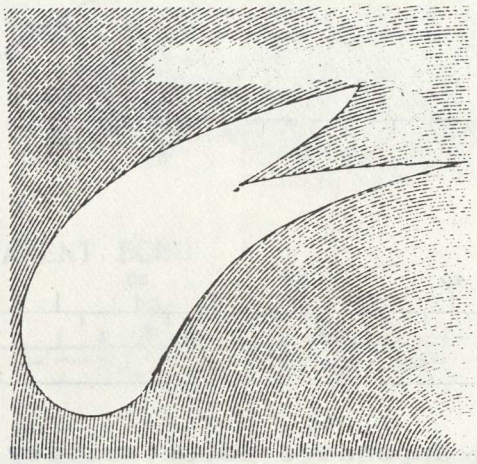

Fig.50. Schematic of "V" notch. (After Whiton and Hamilton, 1976)

10.14 Fingers And Scallops

10.14.1 Definitions

A. Fingers - Finger-like protrusions 2-9 km (1-6 mi) in length.

B. Scallops - Scallops or blunt protuberances 2-5.5 km (1-3 mi) from the edge of a thunderstorm.

10.14.2 Evolution

Harrison and Post (1954) studied fingers and scallops using 5-cm radars on the east slopes of the Rocky Mountains and concluded that rapid changes in shape and intensity of echoes were due to bursts of falling hail.

10.14.3 Radar Characteristics

Fingers and scallops generally protrude from the upwind side of an echo with reflectivities of VIP 5 or VIP 6.

10.14.4 Weather

Hail greater than or equal to 1.3 cm (.5 in) is indicated.

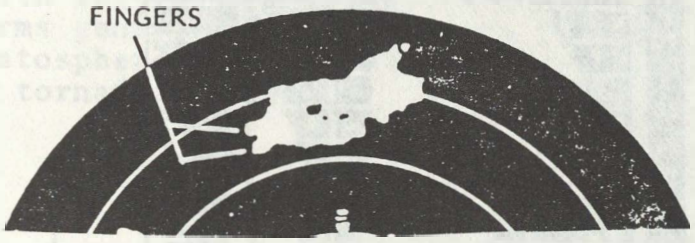

Fig.51. Linear PPI display of hail fingers.

10.15 The Hail Spike

10.15.1 Definition

A narrow echo seemingly extending to 21-24 km (70-80 kft), often exceeding the vertical scale of the range height indicator (RHI).

10.15.2 Evolution

Spikes are caused by side-lobe backscattering from highly reflective targets and are seen on a RHI display only. The spike is a spurious phenomenon with the actual echo tops being lower.

10.15.3 Radar Characteristics

Normal range of detectability is about 56 km (30 nmi) with a maximum range of 157 km (85 nmi).

10.15.4 Weather

Spikes are usually associated with hail and it is suggested that the echo be examined for other severe weather features.

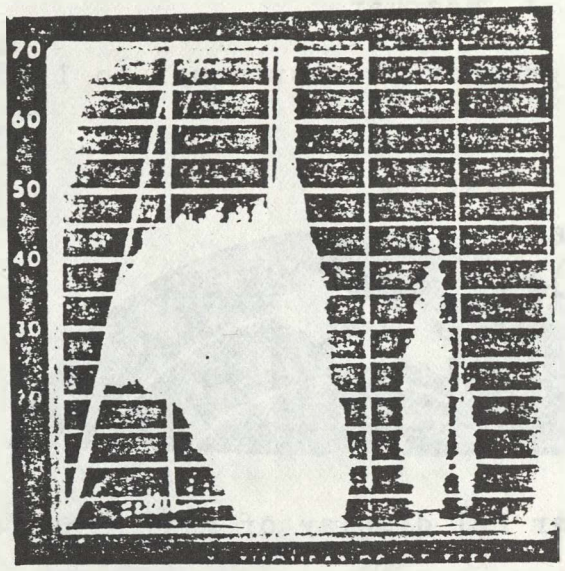

Fig.52. Linear display of RHI spike.

10.16 Echo Tops

The reliability of echo tops is diminished by beam width distortion, abnormal propagation, antenna side-lobe distortions (figure 52), and tops being echo tops and not visual tops. Still, echo top information is useful.

10.16.1 Echo Tops And Severe Local Storms

Bonner and Kemper (1971) found very low critical success indices correlating echo tops with severe weather:

INDICES FOR ECHO TOPS GREATER THAN 10.7 km (35 kft)

	POD	FAR	CSI
Tornadoes	.98	.96	.04
Windstorms	.84	.92	.07
Hailstorms	.91	.94	.06

INDICES FOR ECHO TOPS GREATER THAN 13.7 km (45 kft)

	POD	FAR	CSI
Tornadoes	.63	.94	.06
Windstorms	.57	.89	.10
Hailstorms	.72	.89	.11

10.16.2 Tropopause Penetration By Echo Tops

Williams et al. (1965) found that one-half or more hail-producing storms penetrated the tropopause. Pautz and Doloresco (1963) found that few storms produced tornadoes if they did not penetrate the tropopause. Some penetrations exceeded 6.1 km (20 kft). Average tornado-producing storms

penetrated the tropopause by about 3 km (10 kft) at some point during their life.

In a study by Darrah (1978) it was found that only 19% of thunderstorms with tops of 15 km (49 kft) or more and a tropopause penetration of at least 1.5 km (4,900 ft) were associated with severe weather reports. Also, it was found that hailstorms generally extended 1 km (about 3,300 ft) farther into the stratosphere than windstorms and nearly .8 km (2,600 ft) farther than tornadic storms.

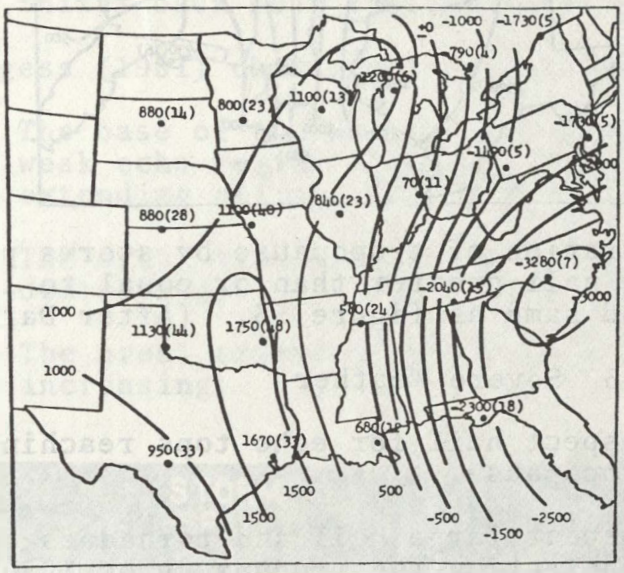

Fig.53. Penetration of tropopause in meters by tornadic storms. Number of cases for each point is given in parentheses. Isopleths of heights are drawn every 500 meters. (After Darrah, 1978)

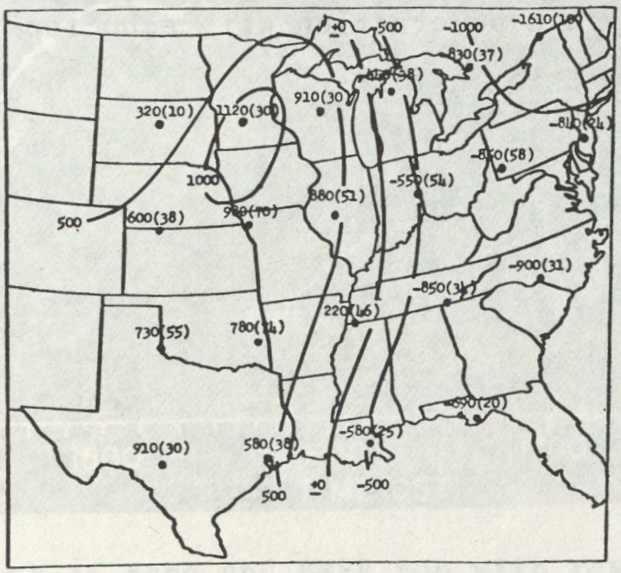

Fig.54. Penetration of tropopause by windstorms greater than or equal to 25 m/s (56 mi/h). Legend same as Figure 53. (Afer Darrah, 1978)

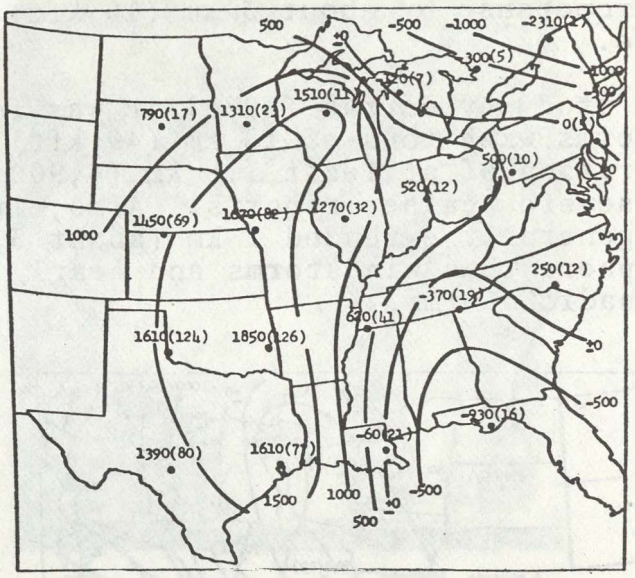

Fig.55. Penetration of tropopause by storms producing large hail greater than or equal to 1.9 cm (.75 in). Legend same as figure 53. (After Darrah, 1978)

10.16.3 Severe Weather

A. Suspect hail for echo tops reaching the tropopause.

B. Suspect large hail and tornadoes for echo tops penetrating the tropopause by 1.5 km (5 kft) or more.

10.16.4 Critical Success Indices

Donaldson et al. (1960) found the following by correlating tropopause penetration with echo tops in New England:

	POD	FAR	CSI
Tornadoes	.83	.89	.10
Windstorms	.75	.95	.05
Hailstorms	.88	.91	.09

10.17 Collapsing Tops

Fujita (1973) noted tornado occurrence after the collapse of overshooting thunderstorm tops.

10.17.1 Radar Characteristics

Lemon (1980) found the echo top generally:

A. Lowers from 2-7 km (about 7-23 kft).

B. Shifts back near the low-level echo core.

Burgess (1981) characterized collapsing tops by:

A. The base of the weak echo region or bounded weak echo region lowering significantly or extending all the way to the ground.

B. The areal extent of the echo at midlevels decreasing.

C. The areal extent of the echo at low levels increasing.

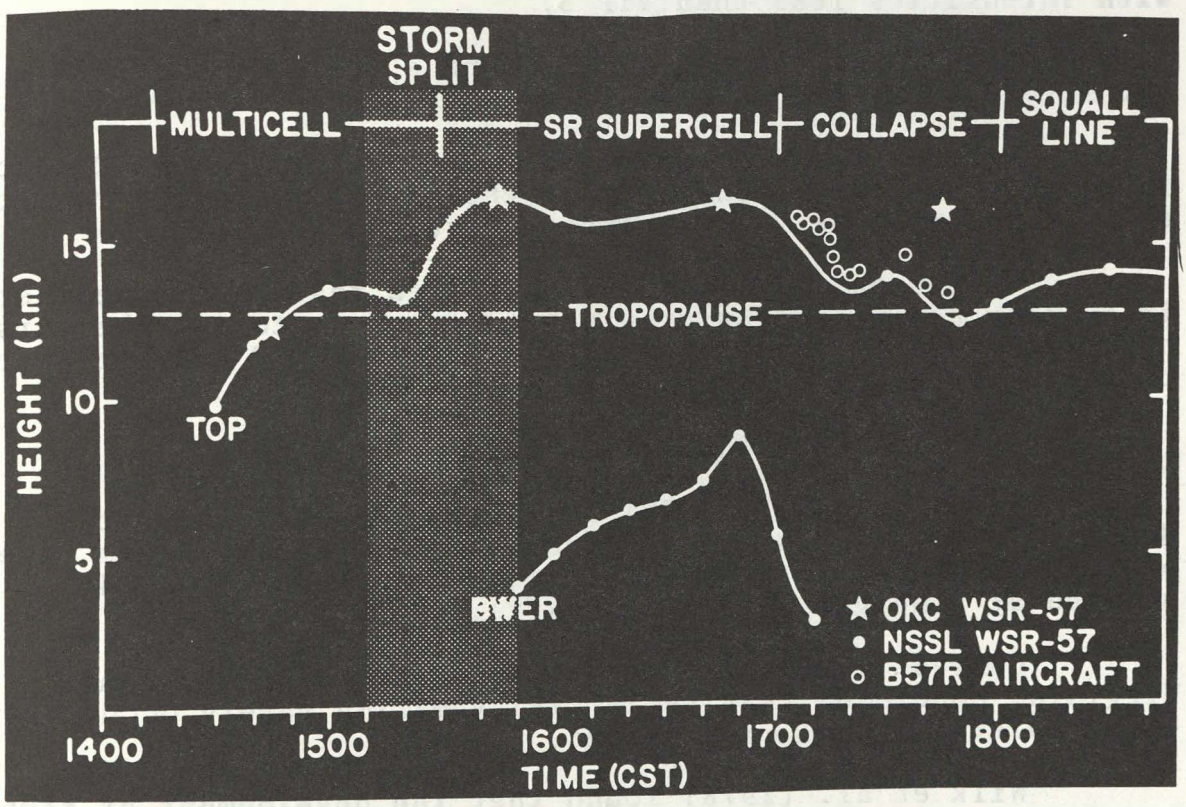

Fig.56. Graph of echo and BWER top with respect to time for a severe thunderstorm in Oklahoma on April 19, 1972. Tornado production began after the BWER started to collapse. (After Burgess, 1974)

10.18 Vaults (Bounded Weak Echo Regions)

The normal maximum range of radar detectability is 130 km (70 nmi). (See "the supercell severe thunderstorm" section beginning on page 20.)

10.19 Echo Reflectivity

10.19.1 Introduction

Different results have been obtained correlating radar reflectivity to storm severity. They are generally due to the wavelength of the radar and the climate of the area investigated.

10.19.2 Low-Level Echo Intensity

Lee (1965) concluded that maximum storm reflectivity is the most reliable indicator of turbulence and that severe turbulence is almost wholly confined to storms with maximum reflectivity of VIP 3 or greater. In general, the tighter the low-level reflectivity gradient, the stronger the updrafts.

Ward et al. (1965) studying hailstorms in Oklahoma with a 10-cm radar found about 85% of all hail falling identified by intensities stronger than VIP 5. Hail was rare and small with intensities less than VIP 3.

Bonner and Kemper (1971) found a POD = .92 and FAR = .82 for severe local storms associated with echoes of VIP 6.

Brandes (1972) studying severe local storms in Oklahoma found that the larger the size of the VIP 2 or greater reflectivity area, the more likely the chance for severe weather.

Whiton and Hamilton (1976) stated that severe weather frequently begins in the growing stages of a storm. The first hail falls 80% of the time before an area of VIP 2 or greater reflectivity reaches its maximum size.

10.19.3 Echo Intensity Aloft

Boyd and Musil (1970) investigating hail in western Nebraska with a 10-cm radar found an optimum false alarm rate of .15 for echoes with a reflectivity threshold of VIP 4 sampled at a height of 3 km (10 kft).

Conrad (1978) studying storms near Wallops Island, Virginia, concluded that reflectivity maxima rarely occur above 4 km (13 kft) in *nonsevere* storms.

Wilk et al. (1978) found that the development of severe local storms as depicted by 10-cm radars begins about 7.4-9 km (24-30 kft) above ground level.

Balsterholt and Lin (1979) in a limited study of 5-cm radar data from the Great Plains during spring and summer found a CSI of .56 for VIP 2 echoes within 1.5 km (5 kft) of the echo top and a CSI of .45 for VIP 4 or greater echoes at a height of 3 km (10 kft) or greater.

11. THROUGH THE PPI LOOKING GLASS

11.1 Radar Past

Conventional radar has been of inestimable value in saving lives and providing advance information of severe local storms since the end of World War II.

11.2 Radar Present

Rinehart (1979) developed a technique for tracking radar echoes by correlation (TREC) which uses conventional radar data to generate Doppler-like motions within storms. This could offer some of the advantages of Doppler radar for today's network of conventional radars.

11.3 Radar Future

The first operational Doppler radars will be installed during the late 1980's. The addition of velocity fields to a conventional radar data base will be of significant value in improving our ability to identify severe local storms.

REFERENCES

Balsterholt, W. H. and Y. J. Lin, 1979: An investigation of radar returns and their relationship to severe weather occurrences. Preprints, 11th Conf. on Severe Local Storms, (Kansas City), Amer. Meteor. Soc., Boston, 193-198.

Bates, F. C., 1963: An aerial observation of a tornado and its parent cloud. Weather, 17, 12-18.

Battan, L. J., 1980: Lightning. McGraw-Hill Encyclopedia of Ocean and Atmospheric Sciences. Sybil P. Parker, Editor in Chief, McGraw-Hill, Philippines, 214-215.

Bigler, S. G., 1955: A comparison of synoptic analysis and composite radar photographs of a cold front and squall line. Proceedings, 5th Weather Radar Conf., Amer. Meteor. Soc., Boston, 113-119.

Bonner, W. D. and J. C. Kemper, 1971: Broad-scale relations between radar and severe weather reports. Preprints 7th Conf. on Severe Local Storms, Amer. Meteor. Soc., Boston, 140-147.

Boyd, E. I. and D. J. Musil, 1970: Radar climatology of convective storms in western Nebraska. Preprints, 14th Radar Meteor. Conf., Amer. Meteor. Soc., Boston, 429-432.

Brandes, E. A., 1972: The use of digital radar data in severe storm detection and prediction. Proceedings 15th Radar Meteor. Conf., Amer. Meteor. Soc., Boston, 45-48.

_____, 1977: Gust front evolution and tornado genesis as viewed by Doppler radar. J. Appl. Meteorol., 16, 333-338.

Brooks, E. M., 1949: The tornado cyclone. Weatherwise, 2, 32-33.

Browning, K. A., 1964: Airflow and precipitation trajectories within severe local storms which travel to the right of the winds. J. Atmos. Sci., 4, 634-639.

_____, 1977: The structure and mechanism of hailstorms. Chapter 1, Hail: A review of hail science and hail suppression. G. B. Foote and C. A. Knight, Ed. Meteor. Monogr., 16, Amer. Meteor. Soc., Boston, 1-39.

Burgess, D. W. (University of Oklahoma, Oklahoma City) 1974: Study of a right-moving thunderstorm utilizing new single Doppler radar evidence. Master's Thesis, 77 pp.

_____, L. R. Lemon and G. L. Achtemeier, 1976: Severe storm splitting and left-moving storm structure. Chapter 6, The Union City, Oklahoma, tornado of 24 May 1973. R. A. Brown, Ed., NOAA Tech. Memo. ERL-NSSL-80, 55.

_____, and R. Davies-Jones, 1977: Unusual tornadic storms in eastern Oklahoma on 5 December 1975. Preprints, 10th Conf. on Severe Local Storms (Omaha), Amer. Meteor. Soc., Boston, 487-492.

_____, R. A. Brown, L. R. Lemon, and C. R. Safford, 1977: Evolution of a tornadic thunderstorm. Preprints, 10th Conf. on Severe Local Storms, Amer. Meteor. Soc., Boston, 84-89.

_____, and R. Donaldson, 1979: Contrasting tornadic storm types. Preprints, 11th Conf. on Severe Local Storms (Kansas City), Amer. Meteor. Soc., Boston, 189-192.

_____, (National Severe Storms Laboratory, NOAA, U.S. Dept. of Comm., Norman, Oklahoma), 1981 (personal communication).

Byers, H. R., and R. R. Braham, 1949: The Thunderstorm, U.S. Government Printing Office, Washington, D.C., 287 pp.

_____, 1974. General Meteorology. McGraw-Hill, New York, N.Y., 4th Edition, 461 pp.

Changnon, S. A., 1977: The climatology of hail in North America. G. B. Foote and C. A. Knight, Ed. Meteor. Monogr., 16, Amer. Meteor. Soc., Boston, 107-128.

Chisholm, A. J. and J. H. Renick, 1972: The kinematics of multicell and supercell Alberta hailstorms. Research Council of Alberta, Hail Studies Report 72-2, 24-31.

_____, 1973: Alberta hailstorms, Part I.: Radar case studies and airflow models. Meteor. Monogr., 14, Amer. Meteor. Soc., Boston, 1-36.

Climatological Data, National Summary, Vol. 4, No. 13, 1980, NOAA, U.S. Dept. of Comm.

Conrad, T. G., 1978: Statistical models of summer rainshowers derived from fine-scale radar observations. J. Appl. Meteorol., 17, 171-188.

Cook, B. J., 1961: Some radar LEWP observations and associated severe weather. Proceedings, 9th Weather Radar Conf., Amer. Meteor. Soc., Boston, 181-185.

Darrah, R. P., 1978: On the relationship of severe weather to radar tops. Mon. Wea. Rev., 106, 1332-1339.

Davies-Jones, R., 1980: Thunderstorm. McGraw-Hill Encyclopedia of Ocean and Atmospheric Sciences. Sybil P. Parker, Editor in Chief, McGraw-Hill, Philippines, 214-215.

Donaldson, R. J., A. C. Chmela, and C. R. Shackford, 1960: Some behavior patterns of New England hailstorms, Physics of Precipitation, Geophys. Monogr. No. 5, Amer. Geophys Union, Washington, D.C., 354-368.

_____, 1965: Methods for identifying severe thunderstorms by radar. Bull. Amer. Meteor. Soc., 46, 174-193.

_____, R. M. Dyer and M. J. Kraus, 1975: An objective evaluator of techniques for predicting severe weather events. Preprints, 9th Conf. on Severe Local Storms, Amer. Meteor. Soc., Boston, 321-326.

English, Marianne, 1973: Alberta hailstorms. Part II. Growth of large hail in the storm. Meteor. Monogr., 14, Amer. Meteor. Soc., Boston, 37-98.

Fankhauser, J. C., I. Paluch, W. A. Cooper, D. W. Breed, and R. E. Rinehart, 1982. Air motion and thermodynamics, Chapter 6, Hailstorms of the Central High Plains, Vol. 1. The National Hail Research Experiment. Colorado Associated University Press (in press).

Fitzgerald, Donald R., 1978: Some relationships of lightning to radar echoes. Aerospace Sciences Review, 78-4, 15-17.

Forbes, G. S., 1978: Three scales of motions associated with tornadoes. U.S. Nuclear Reg. Comm., NUREG/CR-0363 RB, 359 pp.

Fujita, T. and D. C. Bradbury, 1966: Features and motions of radar echoes on Palm Sunday. Preprints, 12th Conf. on Radar Meteorology, Amer. Meteor. Soc., Boston, 319-324.

_____, K. Watanabe, K. Tsuchiya, and M. Shimada, 1972: Typhoon-associated in Japan and new evidence of suction vortices in a tornado near Tokyo. J. Meteor. Soc., Japan, 50, 431-453.

_____, 1973: Proposed mechanism of tornado formation from rotating thunderstorms. Preprints, 8th Severe Local Storms Conf., Amer. Meteor. Soc., Boston, 191-196.

_____, 1978: Manual of downburst identification for project NIMROD. SMRP Res. Paper 156, Univ. of Chicago, 104 pp.

_____, 1979: Objectives, operation, and results of project NIMROD. Preprints, 11th Conf. on Severe Local Storms (Kansas City), Amer. Meteor. Soc., Boston, 259-266.

_____, and R. M. Wakimoto, 1981: Five scales of airflow associated with a series of downbursts on 16 July 1980. Mon. Wea. Rev., 109, 1438-1456.

Galway, J. G., 1967: The use of radar summary charts in SELS operations. National Severe Storms Forecast Center, ESSA, Dept. of Comm., Kansas City, Missouri, 23 pp. (unpublished manuscript).

Goff, C. R., 1976: Vertical structure of thunderstorm outflows. Mon. Wea. Rev., 104, 1429-1440.

Goldman, J. L., 1966: The role of the KuHa-Joukowski force in cloud systems with circulation. Tech. Note 48-NSSL-27, 26.

Hamilton, R. E., 1969: A review of use of radar in detection of tornadoes and hail. Weather Bureau Eastern Region Tech. Memo., WBTM-ER-34. ESSA, Dept. of Comm., 64 pp.

Hammond, G., 1967: Study of a left-moving thunderstorm of 23 April 1964. ESSA Tech. Memo. IERTM-NSSL 31, 75 pp.

Harrison, H. T. and E. A. Post, 1954: Evaluation of C-Band (5.5 cm) airborne weather radar. United Airlines, 108 pp.

Hill, E. L., W. Malkin, and W. A. Schulz, 1966: Tornadoes associated with cyclones of tropical origin-practical features. J. Appl. Meteorol., 5, 745-763.

Hydrometeorological Report #5, 1947: Thunderstorm rainfall. U.S. Dept. of Comm., Weather Bureau.

Kinzer, G. D., 1972: Cloud-to-ground lightning versus radar reflectivity in Oklahoma thunderstorms. NOAA Tech. Memo. ERL-NSSL-59, 24 pp.

Knight, C. A. and N. C. Knight, 1971: Bull. Amer. Meteor. Soc., 52, Feb. issue cover photograph.

Kotov, N. F., 1960: Radiolokatsionnye kharakteristiki livnei i groz. (Radar characteristics of showers and thunderstorms) Leningrad. Glavnaia Geofizicheskaia Observatoriia, Trudy, 102, 63-93.

Lee, J. T., 1965: Thunderstorm turbulence and radar echoes 1964 data studies. ESSA Tech. Note 3. NSSL Report 24, 9-28.

Lemon, L. R., 1976: The flanking line, a severe thunderstorm intensification source. J. Atmos. Sci., 33, 686-694.

_____, 1977: Severe thunderstorm evolution: Its use in a new technique for radar warnings. Preprints, 10th Conf. on Severe Local Storms, Amer. Meteor. Soc., Boston, 77-80.

_____, 1979: On improving National Weather Service severe thunderstorm and tornado warnings. Preprints, 11th Conf. on Severe Local Storms, (Kansas City), Amer. Meteor. Soc., Boston, 569-572.

_____, and C. Doswell, 1979: Mesocyclone and severe thunderstorm structure: a revised model. Preprints, 11th Conf. on Severe Local Storms (Kansas City), Amer. Meteor. Soc., Boston, 458-463.

_____, 1980: Severe thunderstorm radar identification techniques and warning criteria. NOAA Tech. Memo. NWS-NSSFC-3, 60 pp.

McNulty, R. P., D. L. Kelly and J. T. Schaefer, 1979: Frequency of tornado occurrence. Preprints, 11th Conf. on Severe Local Storms (Kansas City), Amer. Meteor. Soc., Boston, 222-226.

Maddox, R. A., C. F. Chappel and L. R. Hoxit, 1979: Synoptic and meso-scale aspects of flash flood events. Bull. Amer. Meteor. Soc., 60, 115-123.

Magor, B. W., 1967: Raob Analysis. National Severe Storms Forecast Center, NOAA, Dept. of Comm., Kansas City, Missouri, 9 pp. (unpublished manuscript).

Mason, B., 1980: Cloud physics. McGraw-Hill Encyclopedia of Ocean and Atmospheric Sciences. Sybil P. Parker, Editor in Chief, McGraw-Hill, Philippines, 99-101.

Moore, C. and B. Vonnegut, 1977: The thundercloud. Physics of lightning. R. H. Golde, Editor. Academic Press Inc., New York, Vol 1, 51-98.

Nelson, S. P., 1976: Characteristics of multicell and supercell hailstorms in Oklahoma. Proceedings, Second WMO Conf. on Weather Modification (Boulder, Colorado), WMO-443, 335-340.

_____, 1977: Rear flank downdraft: A hailstorm intensification mechanism. Preprints, 10th Conf. on Severe Local Storms, Amer. Meteor. Soc., Boston, 521-525.

_____, 1980: Hail production in a supercell-type storm. Proceedings, 3rd WMO Scientific Conf. on Weather Modification (Clermont-Ferrand, France), 655-662.

Newton, C. W. 1963: Movements and patterns of development of thunderstorms, Severe Storm Detection and Circumnavigation, U.S. Dept. of Comm., Weather Bureau, NSSP, Final Report on FAA Contract, ARDS-A-176.

_____, and J. C. Fankhauser, 1964: On the movement of convective storms, with emphasis on size discrimination in relation to water budget requirements. J. Appl. Meteorol., 3, 651-668.

_____, 1968: Convective cloud dynamics - a synopsis. Proceedings, International Conf. Cloud Physics (Toronto, Canada), 487-498.

_____, 1980: Tornado. McGraw-Hill Encyclopedia of Ocean and Atmospheric Sciences. Sybil P. Parker, Editor in Chief, McGraw-Hill, Philippines, 505-506.

Novlan, D. and W. Gray, 1974: Hurricane-spawned tornadoes. Mon. Wea. Rev., 102, 476-488.

Nolen, R. H., 1959: A radar pattern associated with tornadoes. Bull. Amer. Meteor. Soc., 40, 277-279.

Normand, C. W. B., 1946: Energy in the atmosphere. Quart. J. Roy. Meteorol. Soc., 72, 145-167.

Pautz, M., and F. Doloresco, 1963: On the relation between radar echo tops, the tropopause and severe weather occurrences. Proceedings, 10th Weather Radar Conf., Amer. Meteor. Soc., Boston, 51-56.

Pearson, A., 1979: Tornado and severe thunderstorm warning verification. Preprints, 11th Conf. on Severe Local Storms (Kansas City), Amer. Meteor. Soc., Boston, 567-568.

Phipps, C. L. (National Weather Service Southern Region, NOAA, U.S. Dept. of Comm., Fort Worth, Texas), 1979 (personal communication).

Purvis, J. C. and J. F. Sanders, 1981: Hurricane-spawned tornadoes in the South Carolina Coastal Zone. Proceedings, 13th Technical Conference on Hurricanes and Tropical Meteorology (Miami Beach), Amer. Meteor. Soc., Boston.

Rinehart, R. E., 1979: Internal storm motions from a single non-Doppler weather radar. NCAR Tech. Note, NCAR/TN-146+STR, 262 pp.

Sadowski, A., 1969: Size of a tornado warning area when issued on basis of radar hook echo. U.S. Dept. of Comm., ESSA, Weather Bureau, Tech. Memo., WBTM-FCST-10, 26 pp.

Scorer, R. S. and F. H. Ludlam, 1953: Bubble theory of penetrative convection. Quart. J. Roy. Meteorol. Soc., 79, 94-103.

_____, and C. Ronne, 1956: Experiments with convection bubbles, Weather, 11, 151-154.

Smith, J. S., 1965: The hurricane-tornado. Mon. Wea. Rev., 93, 453-459.

Staats, W. F., and C. M. Turrentine, 1956: Some observations and radar pictures of the Blackwell and Udall tornadoes of May 25, 1955. Bull. Amer. Meteor. Soc., 37, 495-505.

Stommel, H., 1947: Entrainment of air into a cumulus cloud. J. Meteor., 4, 91-94.

Stout, G. E. and H. W. Hiser, 1955: Radar scope interpretations of wind, hail and heavy rainstorms between May 27 and June 8, 1954. Bull. Amer. Meteor. Soc., 36, 519-527.

Tecson, J. J., T. T. Fujita and R. F. Abbey Jr., 1979: Statistics of U.S. tornadoes based on the DAPPLE (Damage Area Per Path LEngth) tornado tape. Preprints, 11th Conf. on Severe Local Storms (Kansas City), Amer. Meteor. Soc., Boston, 227-234.

Wallace, J. M., 1975: Diurnal variations in precipitation and thunderstorm frequency over the conterminous United States. Mon. Wea. Rev., 103, 406-419.

_____, and P. V. Hobbs, 1977: Atmospheric Science. Academic Press Inc., New York, N.Y., 467 pp.

Ward, N. B., K. E. Wilk and W. C. Herrman, 1965: WSR-57 reflectivity measurements and hail observations. ESSA Tech. Note 3, NSSL Tech. Memo. 24, 1-8.

Weaver, J. F., 1979: Storm motion as related to boundary layer convergence. Mon. Wea. Rev., 107, 612-619.

Whiton, R. C. and R. E. Hamilton, 1976: Radarscope interpretation: severe thunderstorms and tornadoes. AWS Tech. Rept. No. 76-266, 23 pp.

Wilk, K. E., L. R. Lemon and D. W. Burgess, 1978: Interpretation of radar echoes from severe thunderstorms: A series of illustrations with extended captions, NOAA, Dept. of Comm., National Severe Storms Laboratory, Norman, Oklahoma and National Severe Storms Forecast Center, Kansas City, Missouri, 75 pp. (unpublished manuscript).

Williams, W. E. and Radar Staff, 1965: Radar detection of hail occurrence. Progress Report No. 15, WSR-57 Radar Program, U.S. Weather Bureau, 12-17.

Zittel, W. D., 1978: Echo interpretation of severe storms on airport surveillance radars. Report No. FAA-RD-78-60, National Severe Storms Laboratory, NOAA, U.S. Dept. of Comm., 58 pp.

APPENDIX A

HEIGHT RANGES OF LOW, MID AND UPPER LEVELS

1. INTRODUCTION

Thunderstorms are three dimensional. Therefore, the identification of radar images associated with severe local storms is best accomplished by examining the low, mid and upper levels above ground level (AGL) of the storm. Since the radar beam is usually gaining altitude above the ground with increasing target range, the elevation angle may need to be adjusted to ensure that the operator is looking at a horizontal slice of the atmosphere at a proper level. (See appendix E.)

2. LEVELS

LOW LEVEL: Surface to 1.5 km (4.9 kft) AGL. When the storm is beyond 100 km (62 mi), the lowest scan should be at 0°.

MIDLEVEL: 5-12 km (16-39 kft) AGL.

UPPER LEVEL: Greater than 12 km (39 kft) AGL.

APPENDIX B

RELATIONSHIP BETWEEN VIP INTENSITIES AND DBZ VALUES

1. CONTOURED LOG PLAN POSITION INDICATOR SCHEMATIC DEPICTING SIX LEVELS OF THE VIDEO INTEGRATOR PROCESSOR (VIP)

Fig.B.1

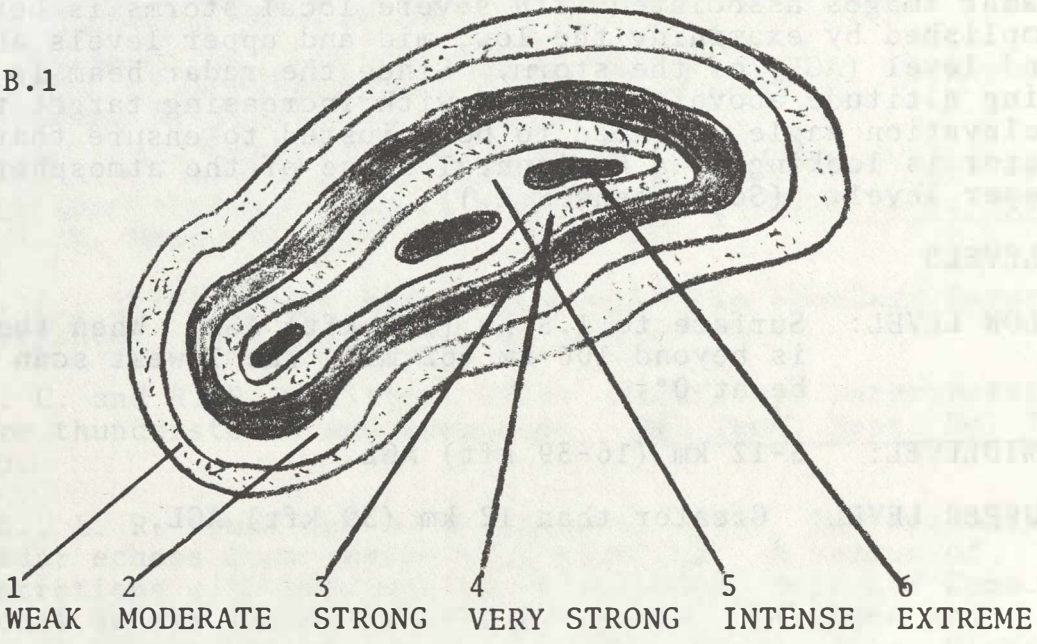

2. VIP-DBZ-CATEGORY-RAINFALL RATE ESTIMATION TABLE

VIP	dBZ	Category	Stratiform (in)	Convective (in)
1	less than 30	Light	less than 0.1	0.05-0.2
2	30	Moderate	0.1-0.5	0.2-1.1
3	41	Heavy	0.5-1.0	1.1-2.2
4	46	Very heavy		2.2-4.5
5	50	Intense		4.5-7.1
6	57	Extreme		greater than 7.1

The stratiform table is based on the relationship, $Z=200R^{1.6}$ and the convective table is based on the relationship, $Z=55R^{1.6}$ where Z represents radar reflectivity and R represents rainfall rate.

APPENDIX C

INDICES USED FOR THUNDERSTORM FORECASTING

1. SHOWALTER

INDEX RANGE	SUBJECTIVE FORECAST
≤ +4	SHOWERS OR POSSIBLE THUNDERSHOWERS
+1 TO -2	THUNDERSTORMS
≤ -3	SEVERE THUNDERSTORMS
≤ -6	TORNADOES

2. K-INDEX

INDEX RANGE	SUBJECTIVE FORECAST
≥ +25	THUNDERSHOWERS

2.1 Definition

K-index is equal to the temperature at 850 mb plus the dewpoint temperature at 850 mb minus the temperature at 500 mb minus the difference between the temperature at 700 mb and the dewpoint at 700 mb.

2.2 Characteristics

2.2.1 The density of the area covered by thundershowers increases with increasing K value.

2.2.2 The K-index is not a good severe local storm forecasting parameter because it is heavily biased towards the existence of moisture at the 700-mb level.

3. TOTAL TOTALS

INDEX RANGE	SUBJECTIVE FORECAST
44-48	THUNDERSHOWERS/THUNDERSTORMS
49-52	SEVERE THUNDERSTORMS
≥ 53	TORNADOES

3.1 Definition

The total totals index is equal to the dewpoint temperature at 850 mb minus the 500-mb temperature plus the temperature at 850 mb minus the 500-mb temperature.

3.2 Characteristic

The dewpoint temperature at 850 mb minus the 500-mb temperature should be greater than or equal to 18.

4. LIFTED INDEX

INDEX RANGE	SUBJECTIVE FORECAST
≤ +4	THUNDERSHOWERS/THUNDERSTORMS
0 TO -3	SEVERE THUNDERSTORMS (WINTER)
≤ -5	SEVERE THUNDERSTORMS (SUMMER)

APPENDIX D

F-SCALE DAMAGE SPECIFICATIONS

1. INTRODUCTION

Fujita (1981) listed categories for damage from tornado or downburst winds.

2. F-SCALE

F0 18-32 m/s (40-72 mi/h)

Light damage. Some damage to chimneys, branches break off trees, shallow-rooted trees push over, sign boards are damaged.

F1 33-49 m/s (73-112 mi/h)

Moderate damage. The lower limit (73 mi/h) is the beginning of hurricane wind speed. Surfaces are peeled off roofs, mobile homes are pushed off foundations or overturned, moving autos are pushed off the roads.

F2 50-69 m/s (113-157 mi/h)

Considerable damage. Roofs are torn off frame houses, mobile homes are demolished, boxcars are pushed over, large trees are snapped or uprooted, light-object missiles are generated.

F3 70-92 m/s (158-206 mi/h)

Severe damage. Roofs and some walls are torn off well-constructed houses, trains are overturned, most trees in a forest are uprooted, heavy cars are lifted off the ground and thrown.

F4 93-116 m/s (207-260 mi/h)

Devastating damage. Well-constructed houses are leveled, structures with weak foundations are blown off to some distance, cars are thrown and large missiles are generated.

F5 117-142 m/s (261-318 mi/h)

Incredible damage. Strong frame houses are lifted off foundations and are carried through considerable distances to disintegrate, automobile-sized missiles fly through the air in excess of 100 m (about the distance along the foul lines to left or right field fences in a major league baseball park), trees are debarked, incredible phenomena will occur.

APPENDIX E

MIDPOINT HEIGHT OF RADAR BEAM UNDER STANDARD ATMOSPHERIC CONDITIONS

1. INTRODUCTION

Lemon (1980) included a schematic showing the approximate height of the midpoint of the radar beam under standard atmospheric conditions. Radar beams tend to be lower during periods of low-level temperature inversions and higher during periods of superadiabatic lapse rates.

2. MIDPOINT HEIGHT OF RADAR BEAM ABOVE GROUND LEVEL

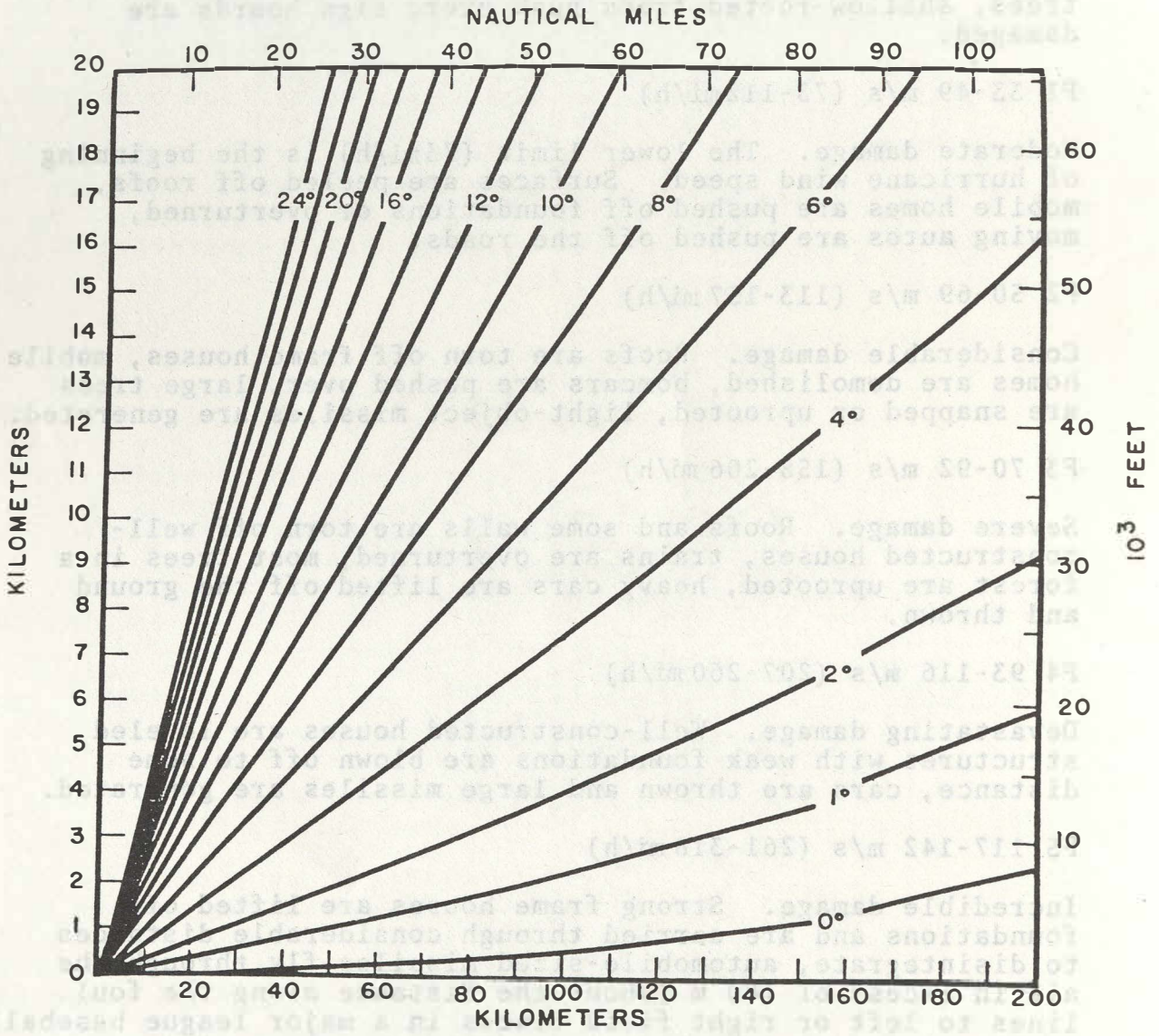

Fig.E.1 Height of the midpoint of the radar beam with the indicated elevation angle and range from the radar. (After Lemon, 1980)

APPENDIX F

RADAR TILT SCAN SEQUENCE

1. INTRODUCTION

According to Lemon (1980), "care must be taken to minimize the time interval between the echo tracings aloft and the low-level comparison scan. If the storm is moving rapidly, an apparent overhang may appear; e.g., on the rear flank, because the low-level echo has moved significantly before the comparison with the midlevel echo and top position."

2. TILT SEQUENCE

2.1

Place a small dot marking the location of a maximum echo top.

2.2

Trace midlevel data to determine the echo overhang using VIP 1. Two or three tracings at different angles may be necessary to determine midlevel overhang.

2.3

Return the antenna to the lowest scan level, 0° when the storm is beyond 100 km (62 mi).

2.4

Compare the low-level echo with the midlevel echo and position of maximum echo top.

2.5

Repeat every 10 to 12 minutes.

APPENDIX G

PROBABILITY OF DETECTION, FALSE ALARM RATIO, AND CRITICAL SUCCESS INDEX

1. INTRODUCTION

Donaldson (1975) introduced a critical success index (CSI). It is defined as the ratio of successful predictions (HITS) to the sum of successful predictions plus the unsuccessful predictions (MISSES) plus the number of false alarms (FALSE ALARMS).

Let us assume your forecast parameter is the hook echo. If you detect a hook echo, issue a warning and a tornado is reported...this is a HIT! If you detect a hook echo, issue a warning and no tornado is reported, this is a FALSE ALARM. A FALSE ALARM does not necessarily mean that a tornado did not form, just that it was not reported. If you do not detect a hook echo and a tornado is reported, this is a MISS.

Table G.1 HIT-MISS-FALSE ALARM TABLE

		FORECAST	
		SEVERE	NONSEVERE
OBSERVED	SEVERE	HIT	MISS
	NONSEVERE	FALSE ALARM	

2. CRITICAL SUCCESS INDEX

$$CSI = \frac{HITS}{HITS + MISSES + FALSE\ ALARMS}$$

A CSI of 1 is perfect, while a CSI of 0 represents utter failure.

Two other indices are useful in calculating your severe weather batting average. They are probability of detection (POD) and false alarm ratio (FAR).

3. PROBABILITY OF DETECTION

POD is the ratio of hits to the sum of hits plus misses:

$$POD = \frac{HITS}{HITS + MISSES}$$

A POD of 1 is perfect, while a POD of 0 represents utter failure.

4. FALSE ALARM RATIO

FAR is the ratio of false alarms to the sum of false alarms plus hits:

$$FAR = \frac{\text{FALSE ALARMS}}{\text{FALSE ALARMS} + \text{HITS}}$$

A FAR of 0 is perfect, while a FAR of 1 represents utter failure.

APPENDIX H

SADOWSKI's TORNADO WARNING TECHNIQUE

1. INTRODUCTION

Sadowski (1969) developed a tornado warning technique based on the circle of best fit for a hook echo detected on a plan position indicator in the linear mode of operation.

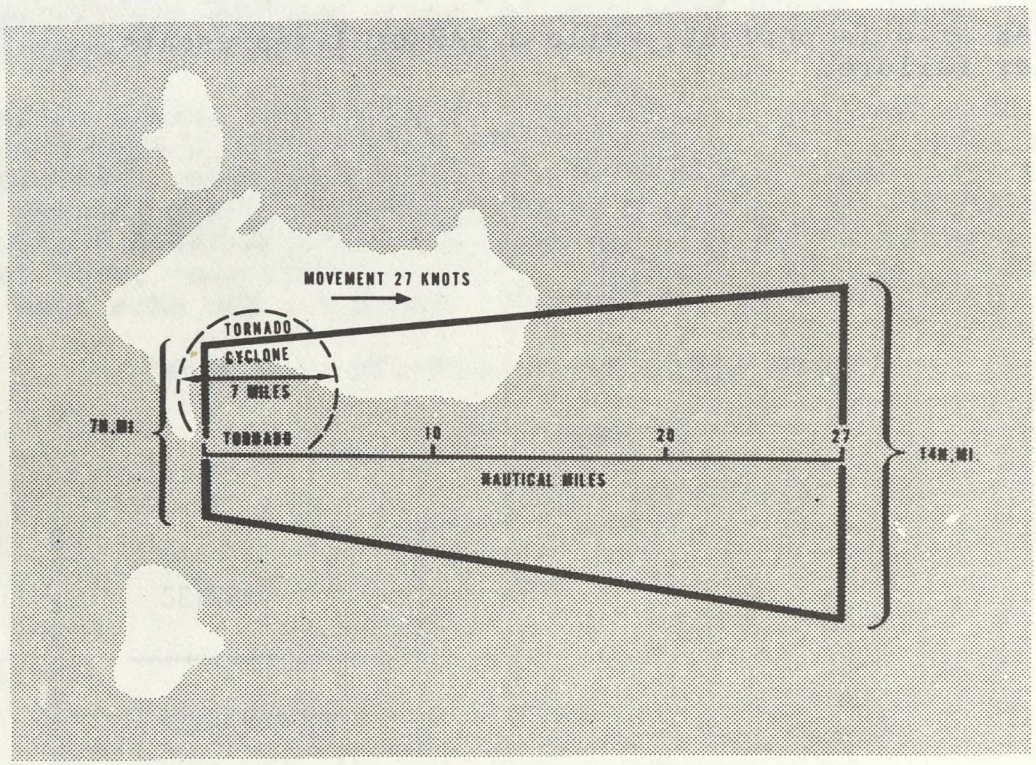

Fig.H.1 Tornado warning area based on circle of best fit for radar hook echo. (After Sadowski, 1969)

2. TECHNIQUE

2.1 Find the circle of best fit of the hook echo.

2.2 Place the center of the circle over the knob end of the hook echo. Draw a diameter at right angles to the direction of movement of the hook.

2.3 Draw a line from the center of the circle at right angles to the diameter; that is, along the direction of movement. The length of the line is equal to the distance the hook will travel in 1 hour. If the speed of the hook is unknown, use an average speed of 30 knots (35 m/h).

2.4 At the end of the path line, draw a line at right angles to it. The length of this line is double the diameter of the circle of best fit. The path line

should bisect the double diameter line.

2.5 Draw lines connecting the ends of the diameter of the circle with the ends of the double diameter line. The result is a truncated triangle and is the area to be warned.

2.6 The duration of the warning is usually 1 hour. A new warning should be issued near the end of the hour if the hook still exists.

2.7 Be reasonable about the use of county boundaries.

APPENDIX I

CONVERSION FACTORS USED IN SELS OUTLINE

1 nmi = 1852 m

1 m = 3.281 ft

1 km = 3281 ft

1 nmi = 6076 ft

1 km = .54 nmi = .62 mi

1 m/s = 2.237 mi/h

1 kg = 2.2046 lb

1 m = 1.094 yd

1 mm = .04 in

1 knot = 1.15 mi/h